Technische Universität München

Fakultät für Medizin

Enhancing CHM1^{319} specific TCR-transgenic T cell cytotoxic effect on Ewing sarcoma cell lines

Emilie Cécile Renée Biele

Vollständiger Abdruck der von der Fakultät für Medizin der Technischen Universität München zum Erlangen des akademischen Grades einer

Doktorin der Medizin

genehmigten Dissertation.

Vorsitz: Prof. Dr. Florian Eyer
Prüfer der Dissertation:

1. Priv.-Doz. Dr. Uwe Thiel
2. Priv.-Doz. Dr. Joseph Mautner

Die Dissertation wurde am 03.03.2023 bei der Fakultät für Medizin der Technischen Universität München eingereicht und durch die Fakultät für Medizin am 15.08.2023 angenommen.

Inhaltsverzeichnis

Abbreviations

ACT	adoptive T cell therapy
AEC	3-Amino-9-ethyl-carbazole
APC	allophycocyanin
APE	apurinic/apyrimidinic endonuclease
CAR	chimeric antigen receptors
CT	computed tomography
CD83L	CD83 ligand
cDNA	complementary DNA
CHM1	chondromodulin 1
cRNA	complementary RNA
DCs	dendritic cells
DMSO	dimethyl sulfoxide
DN	double negative
DNA	desoxyribonucleic acid
DP	double positive
EFS	event free survival
eIF-5A9	eukaryotic initiation factor 5A
EwS	Ewing sarcoma
FACS	fluorescence activated cell sorting
FBS	fetal bovine serum
FISH	fluorescence in situ hybridization
FITC	fluoresceinisothiocyanat
FLU	influenza
GCTB	giant cell tumor of bone
GM-CSF	granulocyte macrophage colony-stimulating factor
GvHD	graft versus host disease
HSV-1	herpes simplex virus 1
ICAM-1	Intercellular adhesion molecule **1**
IFNγ	Interferon gamma
Ig	immunoglobulin
IL-1β	interleukin-1β
IL-10	interleukin 10

IL-4	interleukin 4
IL-6	interleukin-6
imDC	immature dendritic cells
IRF	interferon regulatory factors
iTreg	induced regulatory T-cells
LFA-1	lymphocyte function associated antigen-1
mAB	monoclonal antibody
mCD83	membrane bound CD83
MD-2	myeloid-differentiation-factor-2
mDC	mature dendritic cells
MHC	multi histocompatibility
MRI	magnet resonance imaging
OS	overall survival
PAMPs	pathogen associated molecular patterns
PBS	phosphate buffered saline
PCR	polymerase chain reaction
PD-L1	programmed cell death ligand 1
PD-L2	programmed cell death ligand 2
PE	Phycoerythrin
PET-CT	positron emission tomography - CT
PGE_2	prostaglandin E2
PI	Propidium iodide
rhIL-15	recombinant human interleukin 15
rhIL-2	recombinant human interleukin 2
RNA	ribonucleic acid
sCD83	soluble CD83
SD	standard deviation
TCM	T cell medium
TCR	T cell receptor
TdT	terminal deoxynucleotidyl transferase
TIL	tumor infiltrating lymphocytes
TME	tumor microenvironment
TNF	tumor necrosis factor
UGD	uracil DNA glycosylase

VAC	Vincristine, Actinomycin, Cyclophosphamide
VAI	Vincristine, Actinomycin, Ifosfamide
VEGF	vascular endothelial growth factor
VIDE	Vincristin, Ifosfamide, Doxorubicin, Etoposide
Wt	wild type

List of Figures

List of Tables

Introduction

Paediatric Cancer

Childhood malignancies are the most common cause of death by disease in children aged 12 months and older. According to data of the *Mainz Krebs Register* in Germany, childhood malignancies have an annual incidence of approximately 160 cases per 1.000.000 children with varying incidence numbers among age groups for specific malignancies. The most common childhood malignancies are leukaemia, brain tumors, lymphomas, neuroblastomas, soft tissue sarcomas, nephroblastomas and bone tumors.

Contrary to adult malignancies, endogenous factors such as genetics play a major role in the aetiology of paediatric cancer when compared to exogenous factors.

Despite advances of therapeutic strategies over the past decades, childhood malignancies remain a major cause of death. Hence, further understanding of the underlying pathologies and novel treatment options are required.

Ewing Sarcoma

Ewing Sarcoma (EwS) is a highly malignant small round cell tumor of bone and soft tissue. Following osteosarcoma, Ewing sarcoma is the second most common paediatric bone tumor accounting for 10-15% of all primary bone tumors in children and adolescents with an annual incidence of 0,6/100000 children[13]. The median age of onset is between 10-20 years and the male to female ratio is 1.5:1. The vast majority of cases is seen in Caucasian patients while Afro-Caribbean and Asian populations are considerably less affected. EwS most commonly arise from bone tissue, especially long or flat bones of the lower extremities and the pelvis, yet approximately 10% arise from soft tissue[98].

Genetics

EwS are characterized by the chromosomal rearrangement of the EWSR1 gene located on chromosome 22 and a gene of the ETS family of transcription factors located on chromosome 11[71]. The most frequent chromosomal rearrangement occurring in 85% of cases is the reciprocal translocation t(11;22)(q24;q12) which results in the fusion of the ribosomal binding protein EWS to the transcription factor gene FLI 1 [56, 84, 91, 94]. A fusion of EWS-ERG is seen in 5% of cases while fusions

of EWS to other genes of the ETS family of transcription factors, including ETV1, ETV4, and FEV is found in 3% of cases [59, 64].

The EWS protein is an RNA binding protein incorporating a transcriptional activation domain and an RNA recognition domain at its N-and C-terminus, respectively. The transcriptional activation domain suggests that EWS may act as a transcription factor. Several features of the EWS protein such as its ubiquitous expression, its stability during the cell cycle and the long mRNA half-life suggest that the encoding EWSR1 gene is a housekeeping gene[64].
FLI1 belongs to the ETS family of transcription factors which inherit DNA binding regions at their carboxy termini and can activate specific target genes such as oncogenes or tumor suppressor genes by binding to the corresponding DNA sequence. This group of genes thereby controls a vast number of cellular processes and functions.
The resulting fusion oncogene EWS-FLI1 has been shown to be a major driver of tumor genesis which acts by regulating the expression of genes involved in cancer progression and is highly specific to EwS [29].

Histologically, ESFTs are characterized by small round blue cells. To date, the distinct cell of origin responsible for ESFT has not been identified[91]. However, ESFT gene expression patterns suggest a primitive neural crest-derived progenitor as the cell of origin, as ESFT show similarities to foetal, neuronal and endothelial tissues[76, 90]. It was demonstrated that the neuro-ectodermal differentiation of this progenitor cell is blocked by the overexpression of histone methyltransferase enhancer of Zeste homolog 2 (EZH2) [76, 91]. EZH2 is part of the multiprotein polycomb repressive complex 2 (PRC2) and is known to be highly upregulated in EwS as a direct consequence of the EWS/FLI fusion oncogene[52, 97]. EZH2 is expressed only on proliferating cells and exerts its oncogenic function within the PRC2 complex by methylating lysine 27 on histone 3 (H3K27) and thereby silencing target genes[76, 94]. By suppressing EZH2 expression on established Ewing tumor cell lines, a delay in tumor growth in vivo as well as inhibition of metastatic spread could be demonstrated, most likely to due the resumed cell differentiation [76]. Given its central role in EwS tumor genesis, EZH2 is a prime target in EwS therapy.

Clinical Presentation

Most commonly, the presenting complaint is a diffuse swelling and pain over the affected area which is worse on exertion and may sustain throughout the night. According to the tumor site and size, patients can experience loss of function of the affected limb or joint. In severe cases, patients present with pathological fractures of the affected area. Symptoms also include fever, malaise, and unintentional weight loss[8].

Although EwS can arise in any bone or soft tissue, the site of primary malignancy most frequently involves the pelvis (26 %), the long tubular bones of femur (20%) and tibia (10%) and the chest wall (16%) [8]. Bones that are less frequently affected include spine (6%), bones of the upper extremities (9%) and the skull (2%) [8]. Approximately 10% of EwS arise from soft tissue such as kidneys, breast, GI tract, prostate, endometrium, lungs, adrenal glands and meninges [8].

Due to EwS rapid growth and predisposition to metastasize, about 25% of patients present with metastatic spread at the time of diagnosis, most commonly affecting bone, bone marrow, lung and lymph nodes [8, 41].

Diagnosis

Among others, initial diagnostics include a range of imaging using sonography, computed tomography scans, magnet resonance tomography and positron emission tomography CT. The latter plays a vital role in diagnosis of metastatic disease. Furthermore, baseline diagnostics include a full blood count, differential white blood count and a bone marrow biopsy for conventional cytology and histology. Distinct diagnosis is based on immunohistochemical analysis of a biopsy most commonly obtained via open biopsy of the primary tumor. The presence of small blue round cell tumor and expression of CD99 are considered confirmatory markers for EwS. CD99 is a widely used biomarker which shows a high sensitivity for EwS even though its low specificity render it unreliable as a sole diagnostic marker [3, 84]. Due to common histologic and immunophenotypic features shared with other small round-cell paediatric tumors, extensive immunohistochemical testing may be required for definite diagnosis [8]. In addition, molecular genetic testing is performed to detect the

pathogenic EWS-FLI1 fusion oncogenes using polymerase chain reaction (PCR) or fluorescence in situ hybridization (FISH) [3]. Further tumor staging along the treatment course is conventionally obtained by imaging [17].

Treatment

Following the definite diagnosis and staging of the tumor, multidisciplinary treatment commences with the goal of patient cure. Multimodal therapeutic regimes comprise systemic chemotherapy and local treatment such as surgery, irradiation or a combination of both in individual cases. Evidence suggests that combined modality treatment has a beneficial impact on event free survival, especially in primary disseminated EwS [41].

Over the past decades, the treatment regimens and compositions of chemotherapy directed against EwS have vastly developed but have demonstrated rather gradual improvement of survival rates. One of the most striking advantage was observed upon the incorporation of adjuvant chemotherapy to radiotherapy and surgery as this systematic approach tackled metastatic disease which previous treatment approaches did not[37]. The treatment protocol currently applied along Europe is the Euro Ewing 2012 and reeCur protocol. This protocol entails a primary induction chemotherapy comprised of six cycles of a combination of Vincristine, Ifosfamide, Doxorubicin and Etoposide (VIDE). After the fifth VIDE cycle, a disease evaluation using MRI, CT and PET-CT scans is performed to re-asses tumor progress and plan further local therapeutic action such as surgery, which is conventionally performed following the sixth cycle of VIDE. After that, a randomization into one of three risk groups is performed and the patient receives a further cycle of chemotherapy comprised of either eight cycles Vincristine, Actinomycin and Ifosfamide (VAI) or Vincristine, Actinomycin and Cyclophosphamide (VAC)[8, 105]. In individual cases of the high risk group, e.g. patients presenting with metastatic spread at diagnosis, the treatment with Busulfan-Melphalan high dose chemotherapy followed by autologous stem-cell rescue (BuMel) has recently been subject of investigation, however, so far this treatment option has not shown a distinct advantage when compared to other treatment regimes [25, 31]. Radiotherapy may furthermore be applied prior to surgery or among the courses of VAI/VAC[54]. Histopathological response is determined using the Salzer-Kuntschik Score.

Throughout the past decade, the novel treatment approach of allogenic and autologous stem cell transplantation has been subject of investigation in EwS patients. Studies have shown an improvement in event free survival (EFS) when combining high dose chemotherapy and stem cell transplantation, especially in the subgroups presenting with multifocal disease or relapsed patients [15, 53]. These findings have demonstrated that stem cell transplantation in combination is a feasible yet ineffective option in treatment of EwS. Further investigations and improvements are required, especially regarding toxicity and minimization effects of graft versus host disease (GvHD).

Prognosis

EwS have a five year overall survival (OS) rate of 70-80%, which is significantly reduced to 15% in cases with multifocal primary disease or early relapse (i.e. within 24 months of diagnosis) [91, 96]. The Euro-Ewing clinical trial has reported a 3-year EFS rate of 57-69% and 8-year EFS rates of 47-61% [91]. Prognostic factors include tumor volume, tumor site, patient age, response to initial chemotherapy and metastasis at the time of diagnosis, the latter being the most relevant risk factor [41, 105]. Patients initially diagnosed with isolated pulmonary metastasis have a three year EFS prognosis of >50% compared to a much poorer ten year event free survival prognosis of <10% in patients initially diagnosed with bone or bone marrow metastasis [14]. Despite therapeutic advances and multimodal approach of systemic chemotherapy and local treatment, the relapse rate remains at 30-40%. Early relapse within the first two years of initial diagnosis have a poorer 5 year survival rate of 4% – 8.5% when compared to later recurrence with a 23% – 35% 5 year survival rate [8].

Cancer immunotherapy

T cells form part of the adaptive immune system which major function is to recognize pathogens by binding of the T cell receptor (TCR) to pathogen specific peptides bound to the multi histocompatibility (MHC) complex of antigen presenting cells and thereupon initiate an immune response. Depending on the cell surface protein co-receptor expressed, T cells are categorized into $CD4^+$ T cells (T-helper cells) or $CD8^+$ T cells (cytotoxic T-cells).

T cells originate from bone marrow stem cell precursors that migrate to the thymus where they further mature into $CD4^-$ $CD8^-$ double negative (DN) T cells before they undergo proliferation and differentiation into double positive $CD4^+$ and $CD8^+$ (DP) T-cells[36]. In the next step, DP T cells undergo positive selection mediated by self-MHC molecules expressed within thymal tissue by binding to the TCR with low affinity and mature into single positive $CD4^+$ or $CD8^+$ T cells [30, 36]. If the TCR is unable to bind to MHC molecules, the cells will undergo death by regret. Likewise, if the TCR binds to MHC with high affinity, the cells will undergo programmed cell death initiated by negative selection as they potentially exhibit autoreactive properties (negative selection) [36]. Following positive and negative selection, only about 5% of DP T cells are allowed to transit to the periphery [36]. These T cells are self–MHC restricted which enables them to recognize self-MHC molecules encountered during their thymic development. In addition, they are capable of alloreactivity which allows them to recognize allogenic peptide-MHC complexes that have not yet been encountered during their maturation and initiate severe reactions when encountering these non-self MHC complexes which may clinically manifest as graft versus host disease [30].

In the past decades, cancer immunotherapy and especially adoptive T cell therapy (ACT) with transfusion of tumor infiltrating lymphocytes (TIL) or genetically modified T cells have become an increasingly important factor in oncological therapeutics.
Billingham was the first to describe the process of adoptively acquired immunity in 1954 and thereby laid the groundwork for the novel therapeutic approach[9]. In his work he demonstrated that by infecting a healthy host with tissues from an immunized donor, the healthy host will gain immunity against the transferred tissues. Upon a second exposure to the transferred tissues, the infected host behaved as if it itself has been actively immunized [9]. Hence, the conclusion could be drawn that adoptively acquired immunity can be achieved by transferring immunologically activated tissues such as regional lymph nodes to healthy donors.
This treatment approach was picked up quickly and applied to other medical fields, including oncology. In 1956, Barnes demonstrated improved survival in leukaemia murine models by combining total body irradiation with the transplantation of bone marrow from healthy donors[4]. In 1965, Mathé confirmed the efficacy of anti-leukemic immunotherapy despite lacking essential knowledge regarding donor selection or transplant rejection[66].

Several successful treatment attempts which direct immune responses to recognize and attack tumor cells have been demonstrated [23]. Transferral of haematopoetic cells conjoined with conditioning and immunosuppressive treatment is now an established regime in leukaemia as well as other solid tumors such as melanoma and has yielded great treatment responses[55]. Based on findings of Rosenberg et al. in 1988, the use of TILs is a highly effective treatment option for metastatic melanoma patients[26, 79]. Rosenberg succeeded in establishing tumor regression in those patients by expanding lymphocytes extracted from tumor biopsy in vitro with IL-2 and re-infusing these TILs [79].

Apart from infusion of TILs, another form of ACT was introduced which is based on the generation of genetically engineered antigen-specific T cells directed against proteins overexpressed by various tumoral tissues. Initially designed to address the issue of viral infection following bone marrow transplantation, genetically modified virus-specific T cells generated showed clinical efficacy by mediating antiviral as well as anti-tumoral activity[79]. Studies have satisfactorily demonstrated that the transferred highly specific tumor-reactive T cells were capable of proliferation in vivo that maintained their function and were able to migrate to tumor sites [26].

The success of TIL re-infusion as seen in other malignancies is difficult to apply directly to EwS. One aspect diminishing the efficacy of TIL transplantation in EwS is the fact that EwS, as a paediatric cancer, exhibits a very low number of somatic mutations which is associated with few alterations in cell surface marker expression on tumor cells such as MHC class I marking cells as ‘self’ [38]. In addition, EwS is known as an ‘immunologically cold’ tumor (see tumor microenvironment) as it shows little infiltration with tumor infiltrating lymphocytes when compared to other paediatric malignancies. Furthermore, the use of TIL and virus-specific lymphocytes is limited by the presence of alloreactive T cells which may lead to mild or severe forms of graft versus host disease following transplantation.

In regard to those limitations of TIL therapy in EwS patients, the generation of peptide-specific allorestricted T-cells, that have proven their efficacy in other in other paediatric malignancies such as leukaemia, has been applied to EwS and have yet yielded successful results *in vitro* and *in vivo* (see discussion) [1, 10, 95]. To date, there are two mechanisms by which genetically modified T cells are generated, T cells expressing novel T cell receptors (TCR) or chimeric antigen receptors (CAR) [78]. For

TCR, T cells are isolated in vitro and genetically modified to express TCR that are specific to tumor antigens. It is of note, that a distinct overexpression of that antigen expressed on tumor cells is associated with an increased efficacy of TCR antigen-specific T-cells. However, the expression of MHC class I on tumor cells is required for T cell recognition which poses a limitation to its use as several tumors downregulate the expression of MHC class I over time as an 'immune escape mechanism' [35, 83]. On the other hand, CAR modified T cells are able to exert their anti-tumoral function without MHC class I expression by displaying artificially modified CAR molecules that recognise tumor specific antigens [78].

Tumor Microenvironment

The tumor microenvironment (TME) surrounding tumor tissue has a great impact on tumor genesis and progression. Tumor cells have the ability to manipulate and reprogram their microenvironment by the release of several peptides such as cytokines, chemokines and growth factors which ultimately leads to an environment that favors tumor sustainment and growth[43, 50]. It has become evident that immune cells also add to the composition of TME. Studies imply that these immune cells are altered by cytokines secreted by the TME in order to dampen their immune response directed against tumor progression[28, 43].

Monocyte derived macrophages, which are found within the TME, can be divided into a pro-inflammatory M1 subtype and an immuno-suppressive M2 subtype. By secreting IL-4 and triggering STAT6 signaling in monocyte derived macrophages, the TME promotes the expression of M2 macrophages[43]. M2 macrophages exhibit their immuno suppressive functions by expressing anti-inflammatory cytokines and thereby initiating an inhibitory effect on $CD8^+$ T-cells. In addition, M2 macrophages together with neutrophils are able to promote carcinogenic processes while simultaneously inhibiting anti-tumoral immune responses [91].

Furthermore, by the secretion of immune-suppressive cytokines such as vascular endothelial growth factor (VEGF), interleukin 10 (IL-10), and prostaglandin E2 (PGE2) dendritic cells (DCs) are hindered in their maturation into mature dendritic cells (mDC) and their T cell priming function is impaired[43].

Although the TME of paediatric sarcomas has not been fully explored, it has become evident that the infiltration of inflammatory cells differs among individual sarcomas[50].

Compared to osteosarcoma, undifferentiated pleomorphic sarcoma, and giant cell tumor of bone (GCTB), EwS showed a relatively small infiltration with tumor-infiltrating lymphocytes suggesting a diminished vulnerability towards immunomodulatory therapy [50]. Furthermore, Stahl et al. was able to investigate the composition of the TME of EwS via immunoprofiling analysis and demonstrated that the majority of TILs in EwS are immunosuppressive M2 macrophages (43%) and T cells (23%) [34, 50, 91]. Other immune cells such as B-lymphocytes, plasma cells, and neutrophils were contributed only to a small number of TILs. Further investigations have demonstrated that the majority of T cells infiltrating tumor tissues are $CD8^+$ T-cells[6]. The increased amount of M2 macrophages was associated with a significantly decrease in EFS of 15.3 months compared to a median EFS of 47 months whereas the increased amount of T cells was associated with an improved OS and EFS[91].

The TME is a complex construct orchestrated by the tumor to dampen any immune response directed against tumor progression. Given the many cells involved in the maintenance of the TME, a multitude of cells may be identified as target cells with the common goal of understanding and reversing the immune suppression and reprogramming the immune system to re-establish their immunogenic potency.

CD83

CD83 is a surface marker first reported in 1992 and has since been subject of intense investigation [39, 108]. CD83 is a transmembranous glycoprotein of the immunoglobulin (Ig) superfamily and is primarily known as a highly specific surface marker of mature dendritic cells [39]. In addition, CD83 is expressed on several other activated cells involved in immune responses, including B-lymphocytes, T-lymphocytes, macrophages, and neutrophils [12]. Human CD83 is a highly glycosylated type 1 transmembrane protein mapped to chromosome 6p23 and made up of 186 amino acids. It consists of a C-terminal cytoplasmic tail, a transmembrane domain and an extracellular domain, which is composed of a V-type, Ig-like N-terminal[12, 18]. To date, the transcription factor NF-κB and interferon regulatory factors (IRF) have been identified as responsible pathways regulating CD83 expression upon cell activation [39, 67]. Although the definite mechanism of CD83 processing post-transcription remains uncertain, the RNA-binding protein HuR, eukaryotic initiation factor 5A (eIF-5A9) and nuclear export receptor CRM1 are

proposed to be involved in its transportation from the nucleus [39]. Although specific CD83 interaction partners have been subject to debate in the past, the E3-ubiquitin-ligases of the MARCH-family as well as GRASP5 have been identified to interact with CD83 presented on B-cells and mature dendritic cells, respectively [39].
CD83 has two isoforms, membrane bound CD83 (mCD83) and soluble CD83 (sCD83). Both isoforms differ considerably in their function of regulating immune responses. Although the function of CD83 has not yet been fully understood, CD83 is attributed key immune regulatory functions. As a marker of mature dendritic cells, mCD83 exerts pro-inflammatory action and thereby play a vital role in linking the innate and adaptive immunity. In addition, mCD83 exerts its function as a key immunological director in order to prevent autoimmunity by weakening or regulating over exceeding immune responses [39].

Dendritic cells are derived from myeloid and lymphoid stem cells of the bone marrow and exert different functions according to their maturation status. They form part of the innate immune system and function as one of the most potent antigen presenting cells [22, 39]. Their major role is to initiate a pathogen-specific T cell response by priming naïve T-cells[18, 32].

It has been established that the seven-day cultivation of human peripheral plasma monocytes with interleukin 4 (IL-4) and granulocyte-macrophage-colony-stimulating factor (GM-CSF) under the influence of tumor necrosis factor (TNF) initiates the differentiation into functional $CD83^{+}$ myeloid dendritic cells. Furthermore, a previous study has demonstrated that the differentiation into functional dendritic cells can be triggered by IL-4 alone without GM-CSF although the derived dendritic cells show decreased CD1a expression, which may have a negative impact on their antigen presenting competence [80].

One of the major functions of mCD83 is its role in thymic $CD4^{+}$ T cell differentiation. In 2002, Fujimoto et al. demonstrated in experiments with CD83 knockout mice ($CD83^{-/-}$) that $CD83^{-/-}$ mice exhibited reduced numbers of peripheral $CD4^{+}$ T cells with normal numbers of $CD8^{+}$ T cells when compared to wild type (wt) mice. It was illustrated that a bone marrow transfer from $CD83^{-/-}$ mice to wildtype mice resulted in normal levels of $CD4^{+}$ T cells in wt mice. Furthermore, only a transfer of thymic epithelia cells but not

dendritic cells from wt mice to $CD83^{-/-}$ mice were efficient in rehabilitation of thymic $CD4^+$ T cell differentiation [12, 33, 39, 73]. Taken together, it was demonstrated that sufficient $CD4^+$ T cell differentiation is dependent on the presence of CD83 within the thymic microenvironment. Another study performed later demonstrated that beyond the decrease in quantity, the remaining $CD4^+$ T cells also expressed a weakened response to immune stimulation most likely due to an altered cytokine expression [73]. These findings suggest that the expression of CD83 is vital for the maturation of $CD4^+$ T cells and lack of the surface marker results in decreased number as well as impaired function of $CD4^+$ T-cells. The mechanism of action by which CD83 regulates T cell selection is suggested to be the binding and inhibition of membrane-associated RING-CH8 (MARCH-8) ubiquitin ligase by the transmembrane region of CD83 [60, 63, 104]. Studies have indicated that in thymic epithelial cells, expression of MHC class II is targeted and degraded by MARCH-8. Therefore, by antagonising MARCH-8, CD83 stabilizes the MHC class II cell surface expression on thymic CD4, which is crucial for positive $CD4^+$ T cell selection.

Although CD83 has been shown to regulate $CD4^+$ T cell differentiation, the distinct function of CD83 expressed on activated $CD4^+$ T cell surface has been subject of debate [60]. Previous studies have attributed both immunosuppressive as well as immune stimulatory effects of CD83 on $CD4^+$ T-cells. Studies have shown that CD83 expressed on $CD4^+$ T cells is time-dependent upon TCR activation and that the addition of TGFβ, which is known for its potential to drive the differentiation of naïve $CD4^+$ T cells into induced regulatory T cells (iTreg), maintains CD83 expression. Furthermore, a co-localisation of CD83 and CD25, which forms part of the IL-2 receptor responsible for Treg differentiation, has been observed. Hence, it has been suggested, that continuous CD83 cell surface expression on $CD4^+$ T cells is a potential driver for their differentiation into iTreg cells [22, 39]. One mechanism of action proposed is the binding and inhibition of transmembranous CD83 to the transmembranous portion of E3 ubiquitin protein ligase of the MARCH1-family, which exerts its effect by down regulating surface molecules, including CD25 [22, 99].

Likewise, CD83 expression stabilizes the expression of CD86 and MHC II on B-cells and dendritic cells by inhibiting MARCH1-driven degradation of both CD86 and MHC class II [39, 87]. CD83 is an established marker of B-cells and known to be involved in

B-cell maturation as studies have shown a reduction of B-cells in B-cell specific CD83 knockout mice indicating the correlation between B-cell activation and CD83 expression [12, 39].

Despite being considered the most specific marker of mature dendritic cells, the definite function of CD83 on dendritic cells and T cells remains debatable. Early studies conducted in 1999 indicate one of the major functions of mCD83 on dendritic cells to be their supporting role during T cell activation. The study showed that immature dendritic cells (imDC) infected with herpes simplex virus 1 (HSV-1) expressed decreased numbers of CD83 on their cell surface at maturation and were impaired regarding their function of T cell stimulation indicating its role as T cell enhancer and attributing predominantly pro-inflammatory properties [58, 73, 82]. In addition, more recent studies demonstrated that upon activation, $CD8^+$ T cells express a CD83 ligand (CD83L) on their cell surface which, when interacting with CD83 results in an increase of antigen-specific $CD8^+$ T cells [46].
However, studies obtained with dendritic cells specific CD83 knockout mice demonstrated an overshooting immune response towards pathogens with accelerated killing of bacteria when compared to wt mice most likely due to impaired iTreg regulation [39]. This finding indicated that mCD83 does not solely act as an immune response enhancing agent. In fact, experiments conducted with $CD83^{-/-}$ mice in inflammatory bowel disease expressed increased severity of colitis while an increased CD83 expression showed protective properties against colitis [5]. These findings rather suggest a regulatory role of CD83 in dendritic cell activation and maintenance of homeostasis. Hence, the conclusion was drawn that mCD83 expressed on dendritic cells exerts its immune regulatory functions by promoting T cell activation in order to initiate a proper immune response as well as dampening down overshooting immune reactions to prevent adverse autoimmune disease [39].

On the contrary, sCD83 has been attributed mainly immune suppressive properties. It has become evident that sCD83 dampens the immune response by inhibiting T cell proliferation and T-cell/dendritic cell interaction although the exact underlying mechanism by which it exerts its effect remains unclear. Horvatinovich et al. was able to identify myeloid-differentiation-factor-2 (MD-2), which forms part of the TLR4/MD-2 receptor complex, to be the sCD83 high-affinity binding partner[47]. In general,

following activation by pathogen associated molecular patterns (PAMPs), the TLR4/MD-2 receptor complex dimerises and confers a downstream pro-inflammatory signalling cascade. By the binding of sCD83 to MD-2, the downward cascade is modified so that anti-inflammatory mediators such as IDO, IL-10 and PGE_2 are activated which ultimately leads to T cell proliferation inhibition, unresponsive T-cells, and hindered IL-2 secretion [47, 72]. Given its immunosuppressive properties, sCD83 is a promising therapeutic target especially regarding autoimmune disease and transplant rejection.

Aims

As previously discussed, EwS can be described as immunologically ‘cold’ tumors based on diminished TIL infusion within the tumor microenvironment as well as the predominant M2 macrophage signature detected. Regarding recent advances in immunotherapy in EwS, the goal of this study is to tackle the immunosuppressive TME and thereby enhance the efficacy of anti-tumor agents.

Based on independently acquired previous findings by Thiel et al. and Stahl et al., we assume a biological similarity between EwS cell lines and myeloid cells. Hence, we hypothesize that, like myeloid cells, EwS cells undergo a certain degree of differentiation following the application of specific cytokines commonly used for the generation of CD14 positive myeloid derived dendritic cells. In particular, we hypothesize that the cytokine treatment leads to an upregulation of immunogenic cell surface markers such as CD83, which exhibits pro-inflammatory properties as previously discussed.

The first aim of this study is to verify whether the upregulation of CD83 on EwS cell lines A673, TC71 and SBSR-AKS is reciprocal and if the cytokine application is associated with changes in RNA signature of the treated EwS cell lines.

Furthermore, we attempt to identify the cytokine responsible for a CD83 upregulation as well as the point of time when upregulated CD83 can be detected.

One last aim is to investigate whether an upregulation of CD83 is correlated with the enhancement of chondromodulin 1 (CHM1) TCR transgenic T cell mediated immune response and may therefore potentially qualify as a conditioning regime in EwS treatment.

Materials

Table 1 – List of Manufacturers

Manufacturers	**Location**
Acea Biosciences Inc. / Roche	San Diego, California, USA
Affymetrix	Santa Clara, California, USA
AppliChem GmbH	Darmstadt, Germany
Applied Biosystems	Foster City, California USA
Autoimmun Diagnostika	Strassberg, Germany
B Braun Melsungen AG	Melsungen, Germany
BD Biosciences	San Jose, California, USA
Carl Roth GmbH	Karlsruhe, Germany
Cayman Chemicals	Ann Arbor, Michigan, USA
Corning	Glendale, Arizona, USA
Eppendorf GmbH	Hamburg
Genzeme	Cambridge, Massachusetts, USA
GFL	Burgwedel, Germany
Gibco, Life Technologies	Carlsbad, California, USA
Greiner Bio-One GmbH	Frickenhausen, Germany
Heraeus GmbH	Hanau, Germany
IKA Labortechnik	Staufen, Germany
Implen GmbH	München, Germany
Integra	Biebertal, Germany
Leica Microsystems	Wetzlar, Germany
Mabtech	Nacka Strand, Sweden
Meditrade	Kiefersfelden, Germany
Merck Millipore	Burlington, Massachusetts, USA
Miltenyi Biotec	Bergisch-Gladbach, Germany
Neubauer	Marienfeld, Germany
R&D Systems	Minneapolis, Minnesota, USA
Roth	Karslruhe, Germany
Sarstedt	Nürnbrecht, Germany
Siemens	München, Germany
Starlab	Hamburg, Germany
Systec GmbH	Linden, Germany
Thermo Fisher Scientific Inc	Waltham, Massachusetts USA
TPP	Trasadingen, Switzerland
Wessamat	Kaiserslautern, Germany
Worthington Industries	Columbus, Ohio, USA

Table 2 – List of Instruments and Technical Equipment

Instruments	**Specification**	**Manufacturer**
Autoclave	V95	Systec GmbH
Bag sealer FS 3604	FS 3604	Severin Elektrogeräte GmbH
Cell counting chamber	Neubauer-improved chamber for cell counting	Paul Marienfeld GmbH & Co.KG
Centrifuge	Multifuge 3 S – R	Heraeus GmbH
Centrifuge	5417R	Eppendorf GmbH
Controlled-freezing box 'Mr. Frosty'	Cryogenic freezing container Nalgene™ Cryo 1°c Freezing Container	Sigma-Aldrich GmbH
ELISpot Reader		Autoimmun Diagnostika
Flow Cytometer	MACS Quant 10	Miltenyi Biotec
Freezer -20°C	KG28XM4	Siemens
Freezer -80°C	HLE Series	Thermo Fisher Scientific
Fridge 4°C	KG28XM4	Siemens
Ice machine	Flake-line	Wessamat
Incubator	Hera cell 150	Heraeus GmbH
Liquid nitrogen tank	Level Controller Type	Worthington Industries
Micropipette (0,5 µl - 10 µl, 2 -20 µl, 10 – 100 µl, 20 – 200 µl, 100 - 1000 µl)	Eppendorf plus	Eppendorf GmbH
Microscope	DMIL LED	Leica Microsystems
Multichannel pipette (100 µl)	Eppendorf Research	Eppendorf GmbH
PCR Thermal Cycler		Eppendorf GmbH
Photometer	Nanophotometer	Implen GmbH
Pipette assistant	Pipetboy 2	Integra
Sterile bench	Hera bench	Heraeus GmbH
Thermocycler		Eppendorf GmbH
Vortex	VF2	IKA Labortechnik
Water bath		GFL

Table 3 – List of consumable supplies

Material	**Manufacturer**
Cannulas (0,6x30mm; 0,3x12mm)	B Braun Melsungen AG
Cell culture flask (25 and 75 cm^2)	Greiner Bio-One GmbH
Cell culture plates (12, 24-well)	Techno Plastic Products AG
Cell culture plates (6, 24-well)	Corning Inc.
Cell culture plates (96-well)	Techno Plastic Products AG

Cling film	Via Carl Roth GmbH of Severin Elektrogeräte GmbH & Co. KG
Conical tubes Falcon (15, 50ml)	Greiner Bio-One GmbH
Cryo tubes (1,6ml)	Sarstedt AG & Co. KG
FACS tubes	Corning
Falcon tubes	Greiner Bio-One GmbH
Gloves (latex)	Meditrade
Multiscreen Filter plates	Merck Millipore
Parafilm	Thermo Fisher Scientific Inc
Pipette tips (10, 20, 100 and 100 µl)	Starlab GmbH
Reaction tubes (0,2; 1,5; 2ml)	Sarstedt AG & Co. KG
Serological Pipettes (5, 10 and 25ml)	Greiner Bio-One GmbH
Syringe Filters (0,45µm)	Omnilab Laborzentrum GmbH & Co. KG
Syringes (Original Perfusor 50ml; Omnifix-F 1ml)	B Braun Melsungen AG

Table 4 – List of chemicals and reagents

Chemical / Reagent	**Manufacturer**
AIM-V Medium	Gibco, Life Technologies
BCP (1-Bromor-3-Chloro-Propan)	Sigma-Aldrich GmbH
Bovine serum albumin ≥96%	Sigma-Aldrich GmbH
Dimethylsulfoxide	AppliChem GmbH
Dulbecco's Phophate Buffered Saline (DFBS)	Gibco, Life Technologies
Ethanol	Roth
Ethanol ≥99,8%	Carl Roth GmbH
Fetal bovine serum (FBS)	BD Biosciences
GM-CSF	Genzeme
Human Serum Type AB	Sigma-Aldrich GmbH
IFNγ	R&D Systems
IL-1β	R&D Systems
IL-4	R&D Systems
IL-6	R&D Systems
L-Glutamine 200mM	Thermo Fisher Scientific Inc.
MACSQuant ® Running Buffer	Miltenyi Biotec
MACSQuant ® Washing Solution	Miltenyi Biotec
MACSQuant/MACSima ™ Storage Solution	Miltenyi Biotec
Penicillin-streptomycin 10.000U/ml (100x)	Thermo Fisher Scientific Inc.
PGE_2	Cayman Chemicals
Propidium iodide Solution	Miltenyi Biotec
RPMI-1640 media	Gibco, Life Technologies
TNF	R&D Systems
Trypsin-EDTA 0.5% (10x)	Thermo Fisher Scientific Inc.
Tryptan blue stain (0.4%)	Thermo Fisher Scientific Inc.

Tween-20	Sigma-Aldrich GmbH
X-Vivo medium	Gibco, Life Technologies
Trizol® Reagent	Ambion

Buffer/Solution	**Composition**
FACS Buffer	5 % BSA in PBS
PBS	10% DPBS (10x) in dH_2O
Trypsin	10% Trypsin-EDTA (10x) in dH_2O

Table 5 – Flow Cytometry antibodies

Antibody	**Format**	**Manufacturer**
CD80	PE	Miltenyi Biotec
CD83	APC	Miltenyi Biotec
CD83	APC-Vio770	Miltenyi Biotec
CD86	PE Vio-Blue770	Miltenyi Biotec
HLA-DR	PE	Miltenyi Biotec
ICAM-1	PE	Miltenyi Biotec
Isotypes	FITC/PE/APC-Vio770/Vio-Blue	Miltenyi Biotec
MHC class I	APC	Miltenyi Biotec
MHC class II	APC	Miltenyi Biotec
Mouse IgG1	FITC/PE/APC	BD Biosciences, San Jose, California, USA
PD-L1	FITC	Miltenyi Biotec
PD-L2	APC-Vio770	Miltenyi Biotec
Propidium Iodide Solution	PerCP-Vio700	Miltenyi Biotec

Table 6 – ELISpot and Granzyme B Reagents

Antibody	**Specifictaion**	**Manufacturer**
Capture Antibodies		
Anti-human IFNγ	mAb 1-D1K, purified	Mabtech
Anti-human granzyme B	mAb GB10	Mabtech
Detection Antibodies		
Anti-human IFNγ	mAb 7-B6-1, biotinylated	Mabtech
Anti-human granzyme B	mAb GB11-Biotin	Mabtech
Enzymes and Buffers		
Streptavidin-HRP		Mabtech
3-Amino-9-ethyl-carbazole (AEC)		Sigma-Aldrich GmbH
Peptides		
Gene	**Sequence**	**Sequence**

CHM1	FF302154/1	Thermo Scientific
Influenza	FF334577/1	Thermo Scientific

Table 7 – Cell Culture Media

Medium	**Composition**
Cell culture medium	RPMI-1640 10% FCS 1% P/S 1% Glutamine
Dendritic cell medium	X-Vivo 15 1% human serum type AB
Standard freezing medium	90% FCS 10% DMSO
T cell medium	AIM V Medium 5 % human serum type AB 2 mM L-glutamine 100 U7ml Pen Strep

Table 8 – Commercial Reagent Kits

Kits	**Manufacturers**
The Ambion® WT Expression Kit Invitrogen	Thermo Fisher Scientific
Direct-Zol™ RNA MiniPrep	Zymo Research
GeneChip® WT Terminal Labelling Kit	Affymetrix

Table 9 – Cell lines

Cell line	**Tissue of origin**	**Source**
A673	EwS cell line (type 1 translocation), established from the primary tumor of a 15-year-old girl, p53 mutation	American Type Culture Collection
SBSR-AKS	EwS cell line (type 1 translocation), established from an extraosseous inguinal metastasis of a 17-year old girl (new nomenclature SB-KMS-KS1, originally designated as SBSR-AKS	generated by our laboratory Labor für Krebskranke Kinder der Technischen Universität München

TC71	EwS cell line (type 1 translocation), established in 1981 from a biopsy of recurrent tumor at the primary of a 22-year-old man with metastatic EwS (humerus)	Deutsche Sammlung von Mikroorganismen und Zellkulturen
T2	TAP-deficient hybrid of a T and B lymphoblastic cell line; HLA-A*02:01^{+}, (ATCC CRL-1992)	

Methods

Cell Culturing

All EwS cell lines were cultured in RPMI-1640 medium. Adherent EwS cells lines were cultured in cell culture flasks using RPMI-1640 standard medium at 37°C in a humidified incubator. For 75 cm^2 culture flasks 10ml volume was added, for 25 cm^2 culture flasks 4 ml volume was added. The cells were split every 2 to 4 days according to their individual expansion rate and flask confluence. For detaching the tumor cells, the RPM-1640I medium was removed and cells were washed once using 5 ml phosphate buffered sodium (PBS) before incubating them with at 37°C with 3 ml of Trypsin for 3 minutes. The detached cells were then re-suspended with 7 ml of RPMI-1640 medium and centrifuged at 1300 rpm for 5 minutes before being placed in new cell culture flasks with the respective volume of RPMI-1640 medium.

Suspension cells were cultivated in X-vivo at 37°C. They were split approximately every 5 days at a 1:1 ratio and were re-suspended in 25 ml fresh medium.

To determine the cell number, cells were diluted with trypan blue at a 1:3 ratio. As trypan blue only stains dead cells, viable cells could be detected and counted using a Neubauer counting chamber under a light microscope. Cell concentrations could then be calculated using the following formula:

Cells [number / ml] = number of cells counted x 10^4 x dilution factor [ml]

Freezing and thawing

EwS cell lines were preserved in standard freezing medium at concentrations between 1 x 10^5 and 1 x 10^7 at -80°C. For freezing, the cell lines were centrifuged and the RPMI medium was removed. The cell lines were then re-suspended in 1 ml standard freezing medium and transferred to previously cooled cryovials which were then placed into the controlled freezing boxes for 24 hours before storing them at -80°C.

For thawing, the cryovials were removed from the freezer and stored at 37°C for 5 minutes. The content was washed with RPMI medium, centrifuged, and re-suspended in RPMI medium before being transferred to cell culture flasks.

Culturing tumor cell lines in dendritic cell medium

Three EwS cell lines, A673, SBSR-AKS, and TC71, were cultured in dendritic cell medium. Cells cultured in dendritic cell medium are later termed 'supplememted cells'. On day 0, tumor cells were cultured in 75cm^2 flasks using RPMI medium at a concentration of 5 x 10^5 and 7,5 x 10^5 for A673/SB-SRAKS and TC71, respectively. On day 1, the RPMI medium was removed and 10 ml of dendritic cell medium containing 9,89 ml X-Vivo, 100µl 1% human serum type AB,100µl interleukin-4 (IL-4) and 10µl granulocyte macrophage colony-stimulating factor (GM-CSF). The dendritic cell medium was renewed at the same concentrations on day 3. On day 6, the dendritic cell medium was removed and a maturation cocktail containing 9,89 ml X-Vivo, 100 µl 1% human serum type AB, 20µl interleukin-6 (IL-6), 100 µl interleukin-1β (IL-1β), 10 µl TNF and 10 µl prostaglandin E2 (PGE_2) was added (see concentration in **Figure 1**). One day following the addition of the maturation cocktail, the cells could be utilized for further experiments.

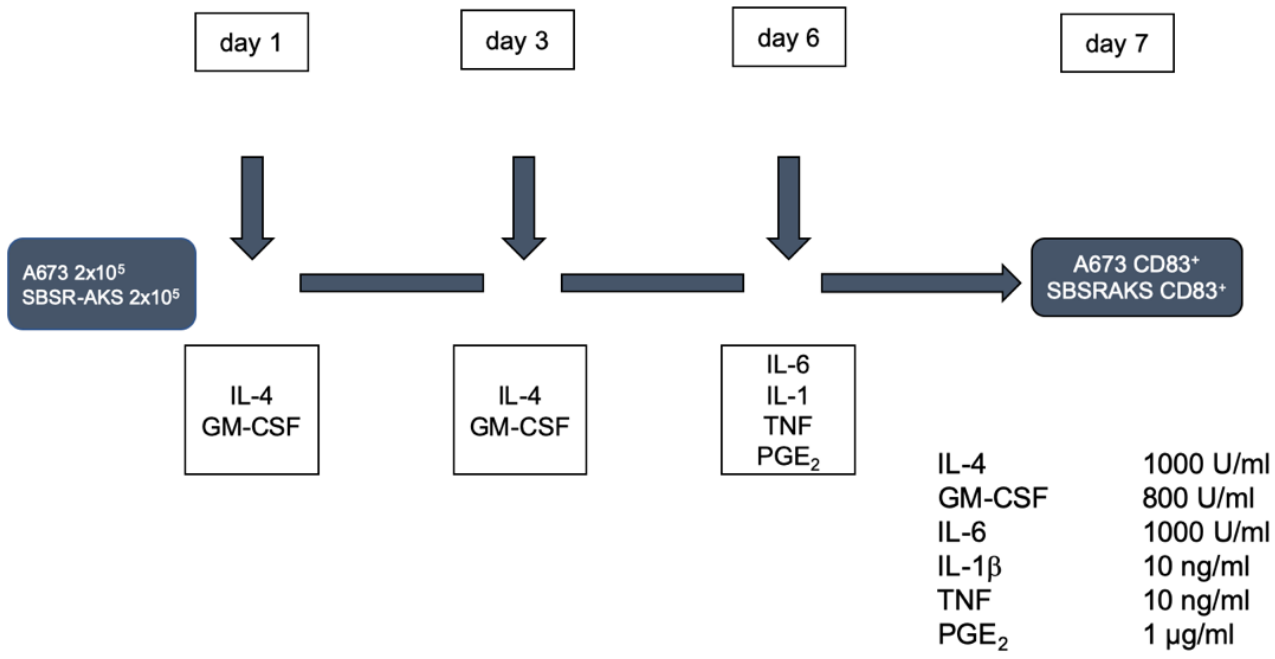

Figure 1 - Dendritic cell medium protocol for culturing EwS cell lines *in vitro* using different cytokines to yield upregulation of certain surface expression markers

ELISpot and Granzyme B

On day 0 of the ELISpot, all adherent tumor cell lines were treated with 100 U/ml interferon gamma (IFNγ) according to the protocol.

On day one, 96-well Multiscreen plates were coated overnight using 10 µl/1ml monoclonal antibody (mAB) 1-D1K (detection of IFNγ) for ELISpot plates and GB10 (detection of granzyme B) for Granzyme B plates.

On day two, previously generated T2-cells were harvested and counted to a concentration of 0,4 x 10^6 T2-cells per 1ml TCM medium. For negative and positive control, 0,5 µl influenza peptide and CHM1 peptide was added to 0,4 x 10^6 cells, respectively. The probes were then vortexed every 15 minutes over two hours while being incubated at 37°C.

The Multiscreen plate was washed using 200 µl PBS and being placed at 4°C for ten minutes after every washing step. This process was repeated four times before the Multiscreen plate was blocked by adding 150 µl T cell medium (TCM) to each well and incubation at 37°C for one hour. In the meantime, T cells were harvested and washed three times with TCM at 1500 rpm for 5 minutes. The T cells were then counted and brought to a concentration of 10.000 or 5.000 cells per 50 µl for the ELISpot. For Granzyme B, we choose the following effector to target ratios: 2.5:1, 0.625:1, 0,156:1 and 0:1. For every ratio, triplicate experiments were performed. After the Multiscreen plate has been blocked, 50 µl with the respective concentration of T cells was added to each well and the plate was incubated for 30 minutes at 37°C. After pulsing of the T2-cells, they were washed twice using TCM and resuspended in 1 ml of TCM. The T2-cells were brought to a concentration of 10000 cells per 50 µl and were stored at 37°C.

The target cell lines were harvested and washed twice using TCM before being counted and being brought to a concentration of 20000 cells per 50 µl.

After incubation of the Multiscreen plate, influenza (FLU) and CHM1 T2-cells and target cells were added carefully to the respective well without manipulating the previously applied T cell volume. The plate was then incubated at 37°C for 20 hours.

On day three, the plate was washed six times using PBS + 0.05% Tween. After thorough removal of PBS + 0.05% Tween, 2 µl/ml detection antibody 7B61-Biotin (ELISpot) and GB11 (Granzyme B) was added prior to incubation at 37°C for two hours. The plate was washed again six times using PBS + 0.05% Tween and incubated with 200 µl streptavidin at room temperature shielded from light exposure for one hour. The plate was washed three times using PBS + 0.05% Tween followed by washing the plate three times with PBS only which was thoroughly removed. 100 µl of development solution containing 3-Amino-9-ethyl-carbazole (AEC) was then added to each well. The

reaction was halted after five to ten minutes by washing the plate using cold water. After drying the plate, the plate was analyzed using the ELISpot reader.

Flow Cytometry

Flow cytometry was performed to analyse the expression of cell surface proteins and detect changes in cell morphology.

Prior to FACS analysis, cell lines were harvested and counted as described previously. The samples were brought to a concentration of 3 x 10^5 in 200 µl PBS per cell line per staining. 200 µl containing the required cell concentration was pipetted to each well of a new 96-well plate, which was centrifuged at 1500rpm for 5 minutes. In the meantime, a master mix containing FACS buffer and the respective FACS isotypes and antibodies was prepared. The cells were resuspended and stained with the according fluorophore-labelled monoclonal antibody in a final volume of 50 µl before being incubated for 30 minutes at 4°C. For every sample a cell sample was stained with the respective isotype control.

After the incubation period, the samples were washed twice with 200 µl FACS puffer and were brought to a final concentration of 200 µl. The samples were then analyzed using the FACS flow cytometry. Dead cells were identified by adding 1 µl of propidium iodide solution (PI) staining seconds prior to FACS analysis.

RNA Isolation and Microarray Analysis

RNA Isolation using Zymo Research Direct-zol™ RNA MiniPrep Kit

Ribonucleic acid (RNA) isolation from both thawed and frozen cells was performed using the Zymo research Direct-zol™ RNA MiniPrep Kit according to the manufacturer's instructions (P/N 9051563).

At first, the cells were harvested, counted and brought to a concentration of 5 – 6 x 10^6 cells diluted in 1ml of TRI Reagent™ Solution and were mechanically crushed using a 23G sized needle before being and incubated at room temperature for five minutes. Per 1ml TRI Reagent™ Solution 100 µl Chloroform was added and probes were incubated at room temperature for 10 minutes before being centrifuged at 4°C at 13000rpm for 20 minutes.

The newly formed clear aqueous RNA phase was then transferred into a Zymo-Spin™ Column provided by the kit and 400µl of 100% ethanol was added before the probes were centrifuged. The probes were then treated with a mastermix containing DNase

and DNA Digestion Buffer and were centrifuged again. Next, the probes were washed twice using Direct-zol™ RNA PreWash followed by centrifugation before the addition of RNA Wash Buffer and the elution step using DNase/RNase-Free Water.
The concentration and quality of the isolated RNA was then obtained by measuring the absorbance of 1 µl of isolated RNA at 260nm using the photometer.

Microarray using Ambion® WT Expression Kit

Alterations in gene expression by cultivating tumor cell lines in dendritic cell medium were detected using microarray analysis.
As described prior, RNA was isolated using the Zymo research Direct-zol™ RNA MiniPrep Kit and the RNA concentration was measured using a photometer at 260nm. If sufficient RNA concentration and RNA quality have been established, the isolated RNA was prepared for whole transcriptome microarray analysis using the Ambion® WT Expression Kit according to the manufacturer's instructions (P/N 900671).
In the first step, single stranded complementary desoxyribonucleic acid (cDNA) was synthesized from total RNA. 200ng of isolated RNA was resuspended in 3 µl H_2O and added to 5 µl of specific engineered primers that contain a T7 promoter sequence before an incubation period using the Eppendorf Cycler of 60 minutes at 25°C, 60 minutes at 42°C and 2 minutes at 4°C. Next, the generated single-stranded cDNA was transformed to double-stranded cDNA by adding a mastermix containing DNA polymerase to generate the double-stranded cDNA and RNase H to degenerated RNA followed by incubating the probes for 60 minutes at 16°C, 10 minutes at 65°C and 2 minutes at 4°C. The double-stranded cDNA then served as a template for antisense cRNA generation and amplification by adding T7 RNA polymerase followed by an incubation period for 60 hours at 40°C. Afterwards, the generated complementary RNA (cRNA) was purified and stabilized by treating the probes with a mastermix containing Nucleic Acid Binding Beads to magnetically separate cRNA from other chemical compounds and then eluting the cRNA from Nucleic Acid Binding Beads by adding elution solution. The amount and quality of the obtained cRNA was measured using a photometer at 260 nm. If sufficient amount and quality was ensured, cRNA would serve as a template for synthesising sense-strand cDNA by reverse transcription using random primers. The probes were then incubated as follows: 5 minutes at 70°C, 5 minutes at 25°C, 2 minutes at 4°C, 10 minutes at 25°C, 90 minutes at 42°C, 10 minutes at 70°C, 2 minutes at 4°C. After cDNA has been synthesized, the cRNA template was

degraded by adding RNase H followed by incubating the probes for 45 minutes at 37°C, 5 minutes at 95°C and 2 minutes at 4°C. The second-strand cDNA was then purified and stabilized as described prior using Nucleic Acid Binding Beads and elution solution. The amount and quality of the purified single-stranded cDNA was again measured using a photometer at 260nm.

cDNA fragmentation and labeling using Affymetrix® GeneChip® WT Terminal Labeling and Hybridization

The fragmentation and labelling of the generated and purified single-stranded cDNA was performed using the Affymetrix® GeneChip® WT Terminal Labelling and Hybridization Protocol according to the manufacturers instruction (P/N 702808).
In brief, for fragmentation of the cDNA, a master mix containing RNase-free water, cDNA fragmentation buffer, uracil DNA glycosylase (UGD) and apurinic/apyrimidinic endonuclease (APE) was added to 5,5 µg of cDNA followed an incubation period of 60 minutes at 30°C, 2 minutes at 93°C and 2 minutes at 4°C. The generated fragmented single-stranded DNA was then labelled by adding a master mix containing terminal deoxynucleotidyl transferase (TdT), TdT buffer and DNA labeling reagent to the fragmented single-stranded DNA and incubating the reactions for 60 minutes at 37°C, 10 minutes at 70°C and 2 minutes at 4°C. Next, a hybridisation cocktail was prepared containing 27 µl of fragmented and labelled DNA, control oligonucleotide B2, hybridisation mix, DMSO and nuclease free water. The hybridisation cocktail was incubated for 5 minutes at 95°C and 45°C, respectively, before injecting 80 µl of the sample into the GeneChip® Probe Array. The arrays were placed in the preheated hybridization oven for 17 hours at 45°C at 60rpm.

Wash step using Affymetrix® GeneChip® Expression Wash, Stain and Scan P/N 702731

The final washing, staining and scanning step of the microarray probes was performed according to the User Guide by Affymetrix® GeneChip® Expression Wash, Stain, Scan Protocol (P/N 702731).
At first, sample files with the according names for every given experiment were set up and registered in the Affymetrix® GeneChip®Command Console. The washing and staining step was performed using the Fluidics Station 450/250 and following the instructions on the LCD window.

After priming the fluidics station, the previously inserted hybridization cocktail was removed and the probes were refilled with 100 µl of a wash buffer (wash buffer A). Next, the stain reagents were prepared by aliquoting 600µl of each staining cocktail one and two and 800µl of array holding buffer and placing the reagents in the according sample holders. After running the washing and staining protocol, the probe cartridge was ejected and inspected for any bubbles and air pockets.

If no bubbles were detected, the probes were scanned using the Affymetrix® GeneChip® Scanner 3000. Prior to its use, the laser of the scanner was heated up for at least ten minutes and the glass surface of the probe array was cleaned. Next, ToughSpots® were applied to both septa of the probe array to prevent fluid loss. The probe arrays were inserted into the scanner and were then scanned using the scan control software according to the protocol.

Statistics

GraphPad Prism (GraphPad Software, San Diego, USA) was used to calculate mean and standard deviation of the mean (SEM). Differences in means between two groups were determined by student's t-test using Microsoft Excel with p-values <0.05 being considered statistically significant.

Results

Cell culturing

Three EwS cell lines, A673, SBSR-AKS and TC71 were cultivated in RPMI-1640 medium alone (control group) or according to the dendritic cell medium protocol (supplemented group) using medium containing X-Vivo, 1% human serum type AB, IL-4 and GM-CSF followed by the addition of a maturation cocktail containing IL-6, IL-1β, TNF and PGE_2 for a total of seven days (see **Figure 1**). This regime was conducted prior to all experiments.

Following the addition of the maturation cocktail, spherocyte formation and detachment of cells from the flask could be observed in all cell lines to varying extents. TC-71 EwS cells showed distinct detachment with insufficient viable cells remaining hence rendering the cell line unsuitable for further experiments.

FACS analysis demonstrating cell surface expression

CD83

On day seven, we assessed the cell surface profiles of A673 and SBSR-AKS cells cultivated in dendritic cell medium (supplemented group) compared to A673 and SBSR-AKS cells cultivated in RPMI-1640 medium (control group) by flow cytometry analysis. We observed a marked upregulation of surface CD83 expression in both cell lines in the supplemented group compared to the control group (see **Figure 2**). For analysis, we used both APC fluorophore antibodies as well as APC-Vio770 fluorophore antibodies. The upregulation of CD83 was reciprocal and seen with either antibody staining.

CD80, CD86, HLA-DR

In order to evaluate a hypothetical similarity to or differentiation of EwS cells into cells of the myeloid department, we further evaluated other markers of mature dendritic cells CD80 (PE), CD86 (VioBlue) and HLA-DR (PE) and their expression on A673 and SBSB-AKS after cultivation in dendritic cell medium. For the SBSR-AKS cell line, our experiments demonstrated no marked upregulation of any of the mentioned cell surface markers between the supplemented group and the control group (data not shown). For the A673 cell line, we observed minor upregulations in CD80 and CD86 cell surface expression and more definite upregulation of HLA-DR surface expression

when comparing A673 supplemented group to A673 control group (see Appendix). These observed increases in upregulation, however, were not as distinct as the CD83 upregulation observed.

MHC class I and II

In both A673 and SBAR-AKS cell lines, we observed an upregulation of surface expression of MHC class I (APC) with supplemented groups compared to control groups. MHC class II upregulation could not be observed on cell surface of either cell line.

ICAM-1, PD-L1 and PD-L2

The expression of intercellular adhesion molecule 1 (ICAM-1) (PE) was upregulated in both A673 and SBSR-AKS cell lines in the supplemented groups compared to the control groups. In A673, the expression of programmed cell death ligand 1 (PD-L1) (PE) was only slightly upregulated in the supplemented group but not in SBSR-AKS. Programmed cell death ligand 2 (PD-L2) (APC-Vio770) surface expression was not elevated in either EwS cell line (see **Figure 2**).

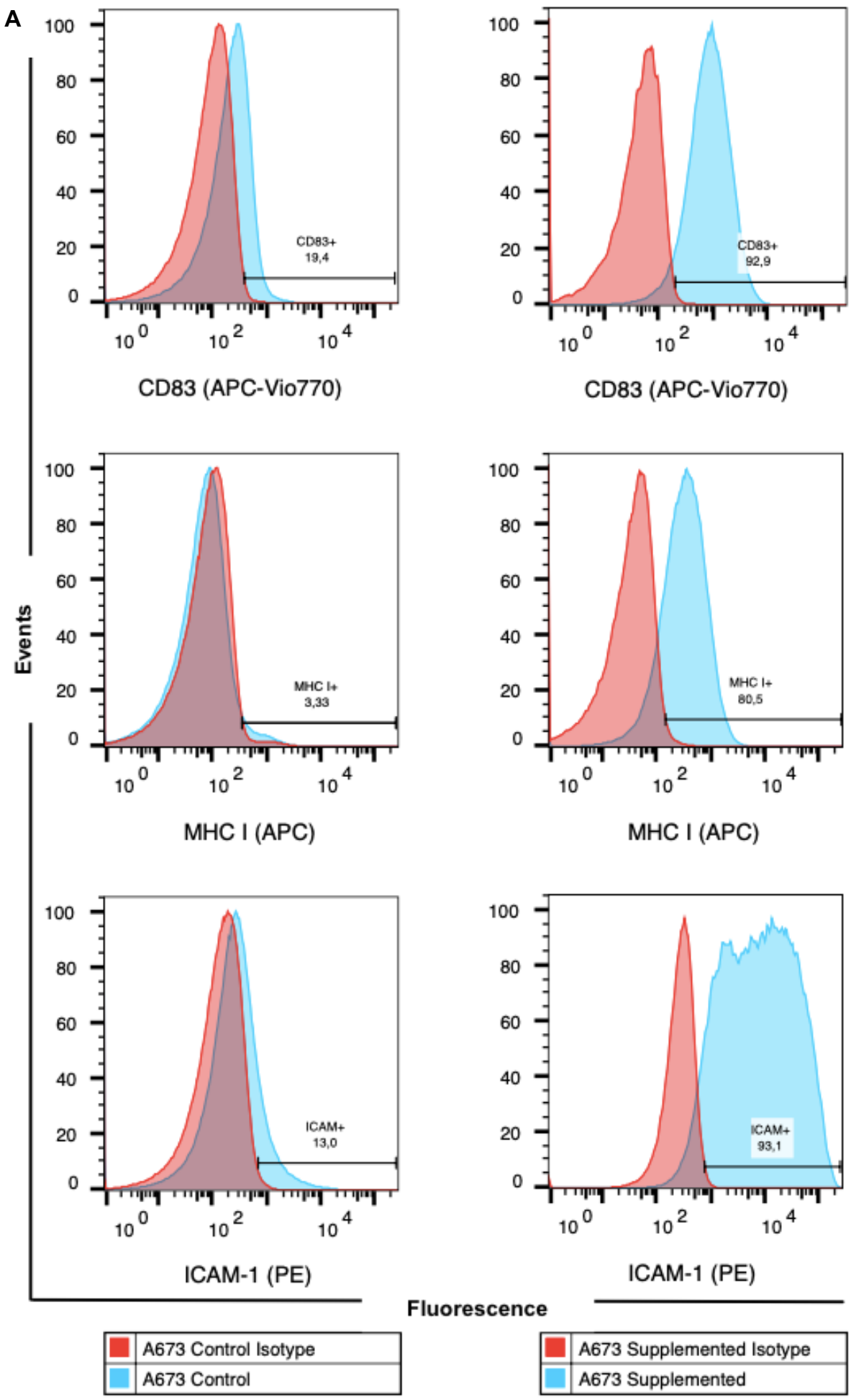
A
Events
CD83+
19,4
CD83 (APC-Vio770)
CD83+
92,9
CD83 (APC-Vio770)
MHC I+
3,33
MHC I (APC)
MHC I+
80,5
MHC I (APC)
ICAM+
13,0
ICAM-1 (PE)
ICAM+
93,1
ICAM-1 (PE)
Fluorescence
A673 Control Isotype
A673 Control
A673 Supplemented Isotype
A673 Supplemented

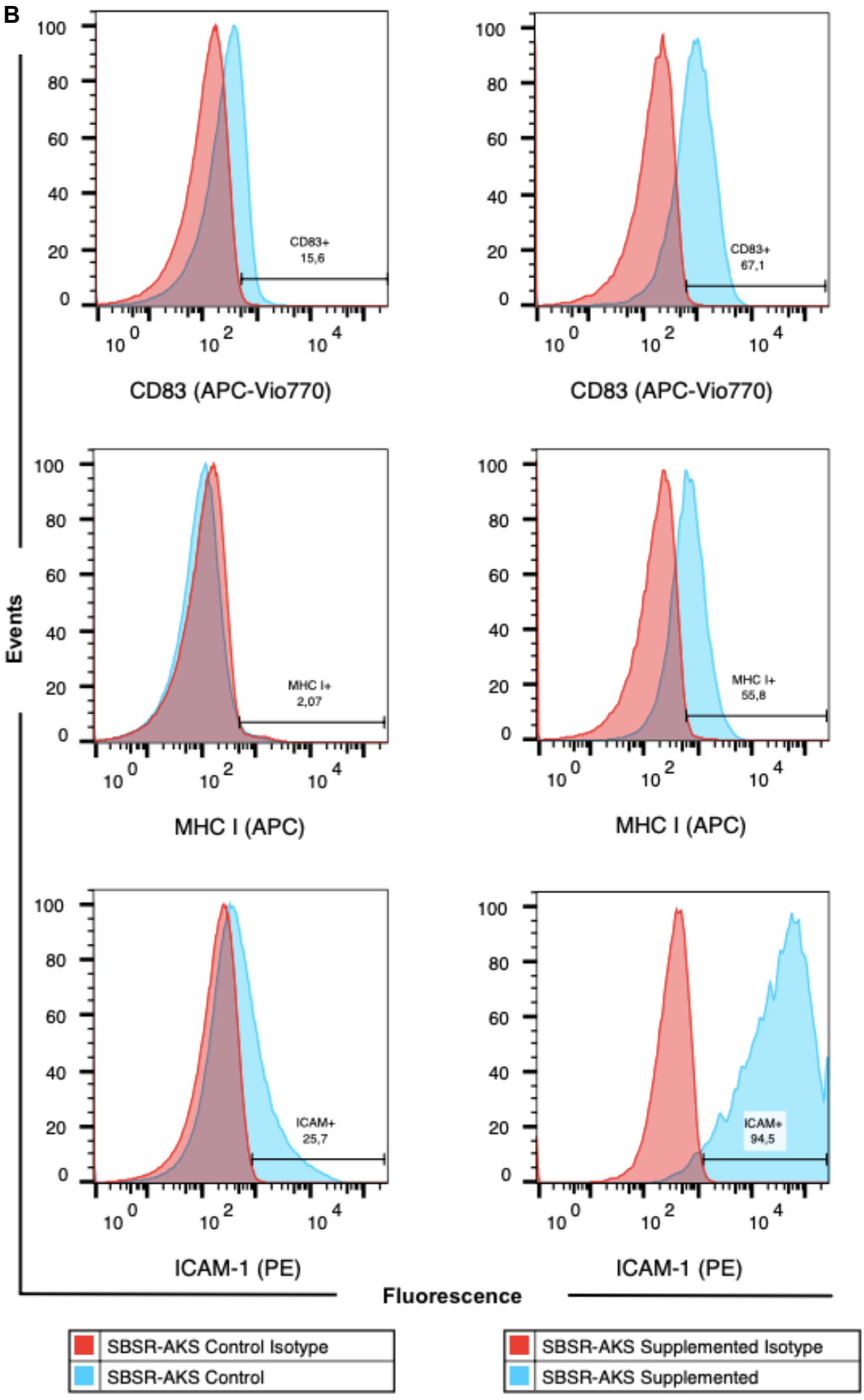
B
Events
CD83+
15,6
CD83 (APC-Vio770)
CD83+
67,1
CD83 (APC-Vio770)
MHC I+
2,07
MHC I (APC)
MHC I+
55,8
MHC I (APC)
ICAM+
25,7
ICAM-1 (PE)
ICAM+
94,5
ICAM-1 (PE)
Fluorescence
SBSR-AKS Control Isotype
SBSR-AKS Control
SBSR-AKS Supplemented Isotype
SBSR-AKS Supplemented

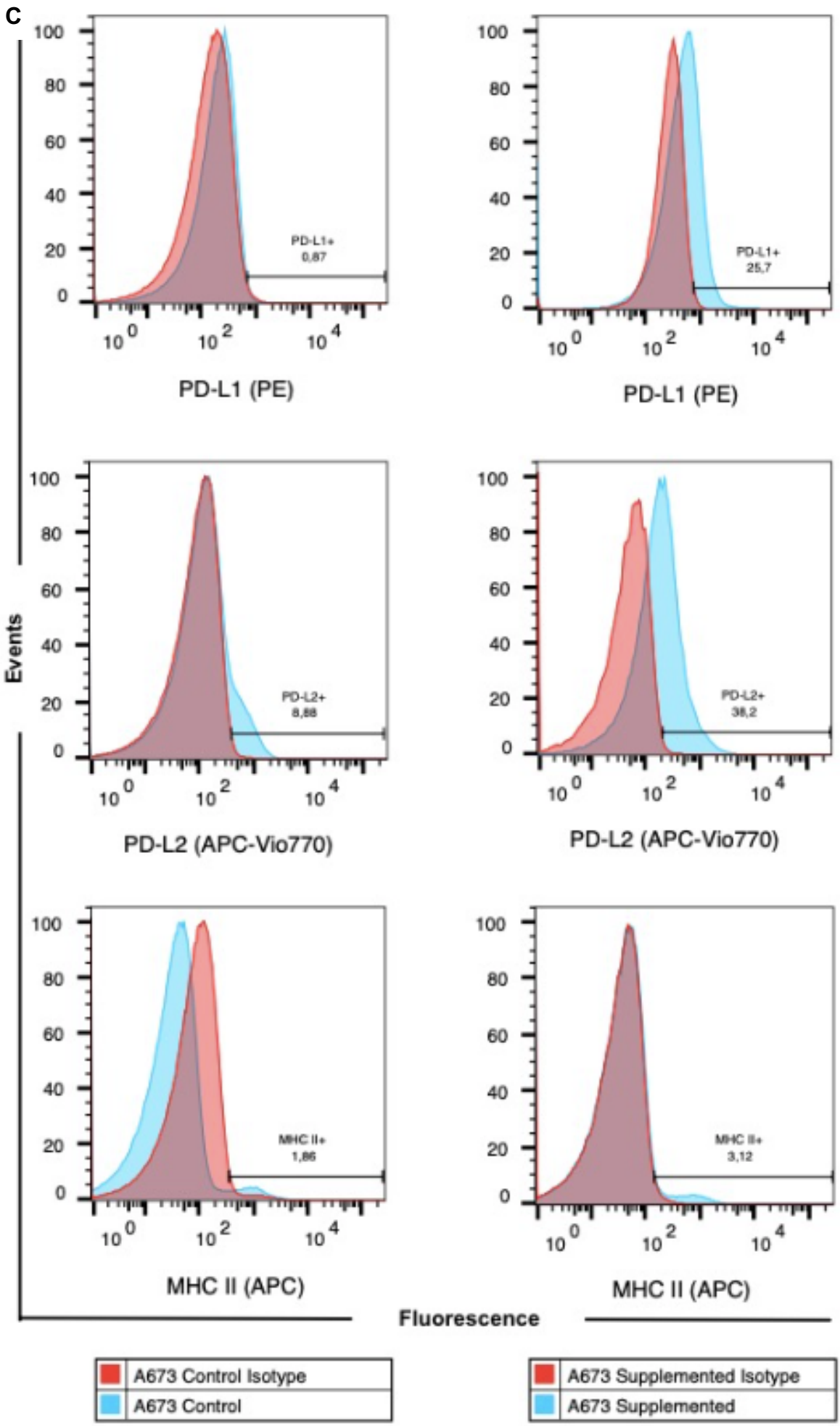
C
Events
PD-L1+
0,87
PD-L1 (PE)
PD-L1+
25,7
PD-L1 (PE)
PD-L2+
8,88
PD-L2 (APC-Vio770)
PD-L2+
38,2
PD-L2 (APC-Vio770)
MHC II+
1,86
MHC II (APC)
MHC II+
3,12
MHC II (APC)
Fluorescence
A673 Control Isotype
A673 Control
A673 Supplemented Isotype
A673 Supplemented

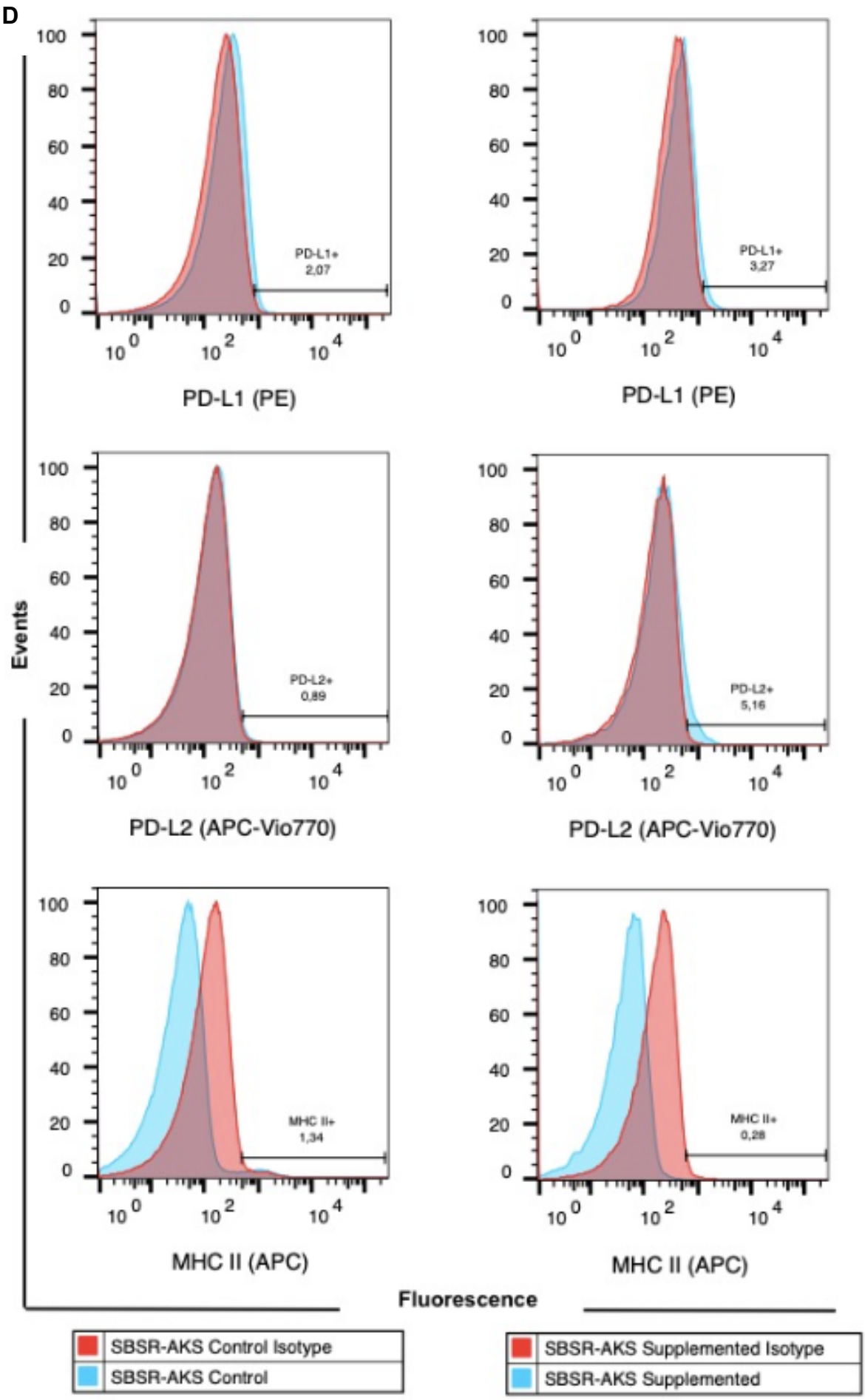
D
Events
PD-L1+
2,07
PD-L1 (PE)
PD-L1+
3,27
PD-L1 (PE)
PD-L2+
0,89
PD-L2 (APC-Vio770)
PD-L2+
5,16
PD-L2 (APC-Vio770)
MHC II+
1,34
MHC II (APC)
MHC II+
0,28
MHC II (APC)
Fluorescence
SBSR-AKS Control Isotype
SBSR-AKS Control
SBSR-AKS Supplemented Isotype
SBSR-AKS Supplemented

Figure 2 – Flow Cytometry Data. Two groups, control group (red histogram) cultured in standard medium and supplemented group (blue histogram) cultured in dendritic cell medium were compared. Gates were set according to the IgG-isotype control (red histogram) and compared to the antibody-labelled cells (blue histogram). **A)** A673 CD83, MHC class I and ICAM-1 expression is upregulated in supplemented (right) versus non-supplemented control cells (left). The gates were set according to isotype-labelled control samples. **B)** SBSR-AKS CD83, MHC class I and ICAM-1 expression is upregulated in supplemented (right) versus non-supplemented control cells (left). **C)** A673 PD-L1, PD-L2 and MHC class II expression comparing control and supplemented groups. PD-L1 and PD-L2 expressions are slightly upregulated. **D)** SBSR-AKS PD-L1, PD-L2 and MHC class II expression comparing control and supplemented groups. There was no observed upregulation observed in either of the three surface markers.

RNA Microarray Analysis

We performed microarray analysis of A673 and SBSR-AKS EwS cell lines comparing the supplemented group with the control group in order to identify possible changes on genomic level. Analysis and visualization of results was conducted with the iSEE software. The generated heatmap illustrating the difference of gene expression between the supplemented group and the control group demonstrates an overall congruency of both independently tested A673 cell lines (see **Figure 3**). The genes expressed by the heatmap represent various agents involved in immune responses. The most important findings are listed below (see **Figure 4**).

CD83

Our Microarray analysis demonstrated an increase of CD83 in both A673 and SBSR-AKS cell lines cultivated according to the dendritic cell medium protocol when compared to the control groups hence supporting the data obtained by flow cytometry (see **Figure 4**). However, it has not be noted, that the increase of CD83 upregulation observed in A673 cell line is much more distinct than the observed upregulation in SBSR-AKS cell lines which differs from findings observed by flow cytometry, where the observed CD83 upregulation was relatively similar. The findings of CD83 upregulation demonstrated in the A673 supplemented group were fairly similar in two separately conducted measurements.

MHC class I and II

In both cell lines cultivated in dendritic cell medium, we observed an upregulation of MHC class I on RNA level which is in line with our findings obtained by flow cytometry. Likewise, we could not observe an upregulated expression of MHC class II in either A673 or SBSR-AKS cell line (see **Figure 4**).

ICAM-1, PD-L1 and PD-L2

For both cell lines cultivated in dendritic cell medium, the expression of ICAM-1 is markedly upregulated when compared to the control group. Likewise, the expression of PD-L1 is upregulated in A673 and SBSR-AKS in the supplemented groups (see **Figure 4**). For A673 cell line, these findings are in line with our findings obtained by flow cytometry. Overall, the expression of PD-L2 is increased in both cell lines in the supplemented groups although to varying extents.

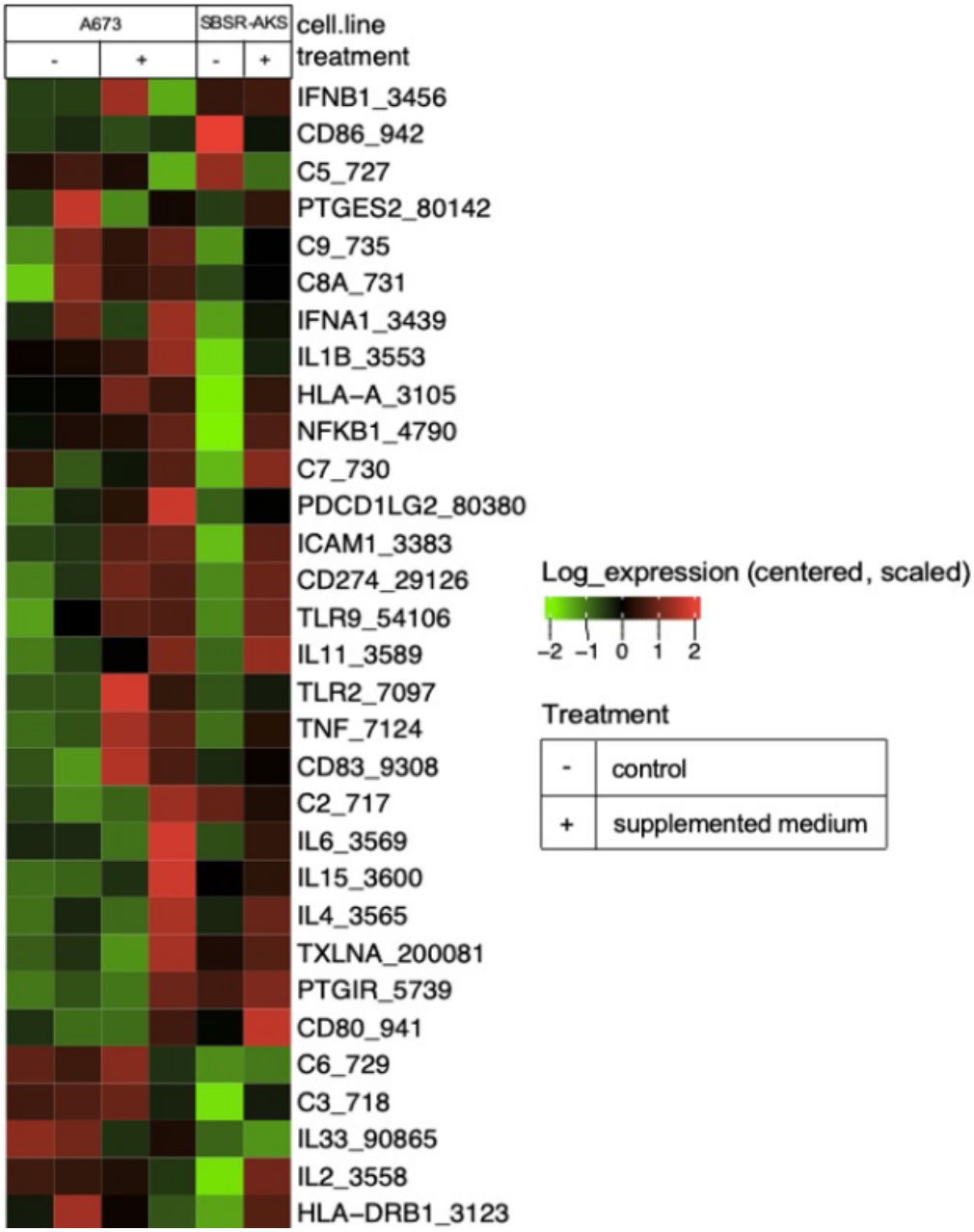

Figure 3 - Heatmap demonstrating expression of various genes involved in immune responses. This heatmap compares the difference in expression of two ES cell lines A673 and SBSR-AKS that were cultivated in standard medium (- / control) or dendritic cell medium (+ / supplemented).

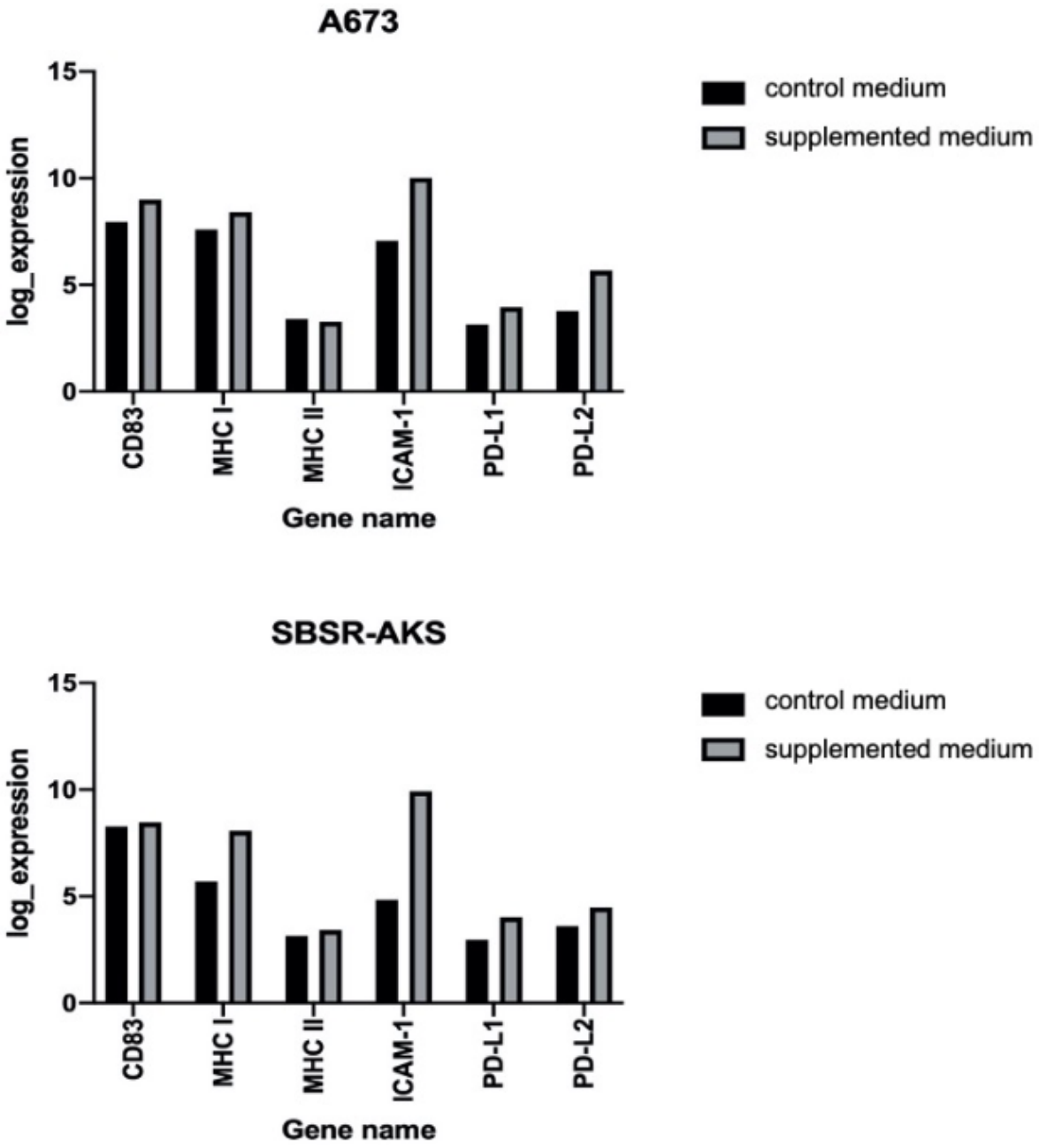

Figure 4 - RNA expression of CD83, MHC class I, MHC class II, ICAM-1, PD-L1 and PD-L2 on A673 and SBSR-AKS ES cell lines obtained by Microarray analysis. This figure demonstrates the difference on gene expression between the control group and the supplemented group.

Identification of driver cytokines by flow cytometry

In order to identify the driver cytokine responsible for the upregulation of CD83 cell surface expression on A673 cell lines, we performed three different experimental approaches which were all obtained by altering the maturation cocktail on day six of the dendritic cell maturation protocol (see **Figure 1**). In the first experiment, we added only one of the four cytokines of the maturation cocktail on day six (‘only one’). In a further experiment, we only added three out of the four cytokines that make up the maturation cocktail on day six (‘minus one’). Finally, we conducted an experiment during which we cultivated the tumor cells in single dose cytokine concentration as well as increasing the dose of each cytokine individually as well as the full maturation cocktail by five-fold.

Addition of single cytokine

The effect on CD83 expression of adding a single cytokine of the maturation cocktail on day six was analyzed by flow cytometer analysis. As seen in **Figure 5** and **Figure 6**, all groups i.e. every cytokine used as a sole mediator, demonstrates an upregulation of CD83 (APC-Vio770) on cell surface although to varying extent. As demonstrated in **Figure 5**, the CD83 expression was most distinctly upregulated with single use of TNF when compared to single use of other cytokines. When comparing the extent of CD83 upregulation observed by use of TNF only versus use of the full maturation cocktail, there is no distinct difference between both treatment groups indicating similar effects on upregulation of CD83 surface expression.

Addition of three out of four cytokines

The effect of adding three out of four cytokines of the maturation cocktail on day 6 was analyzed by flow cytometry and is displayed in **Figure 5.** In contrast to the addition of a single cytokine, these findings do not distinguish one treatment group to be the most effective in CD83 (APC-Vio770) upregulation but a roughly similar upregulation among all groups.

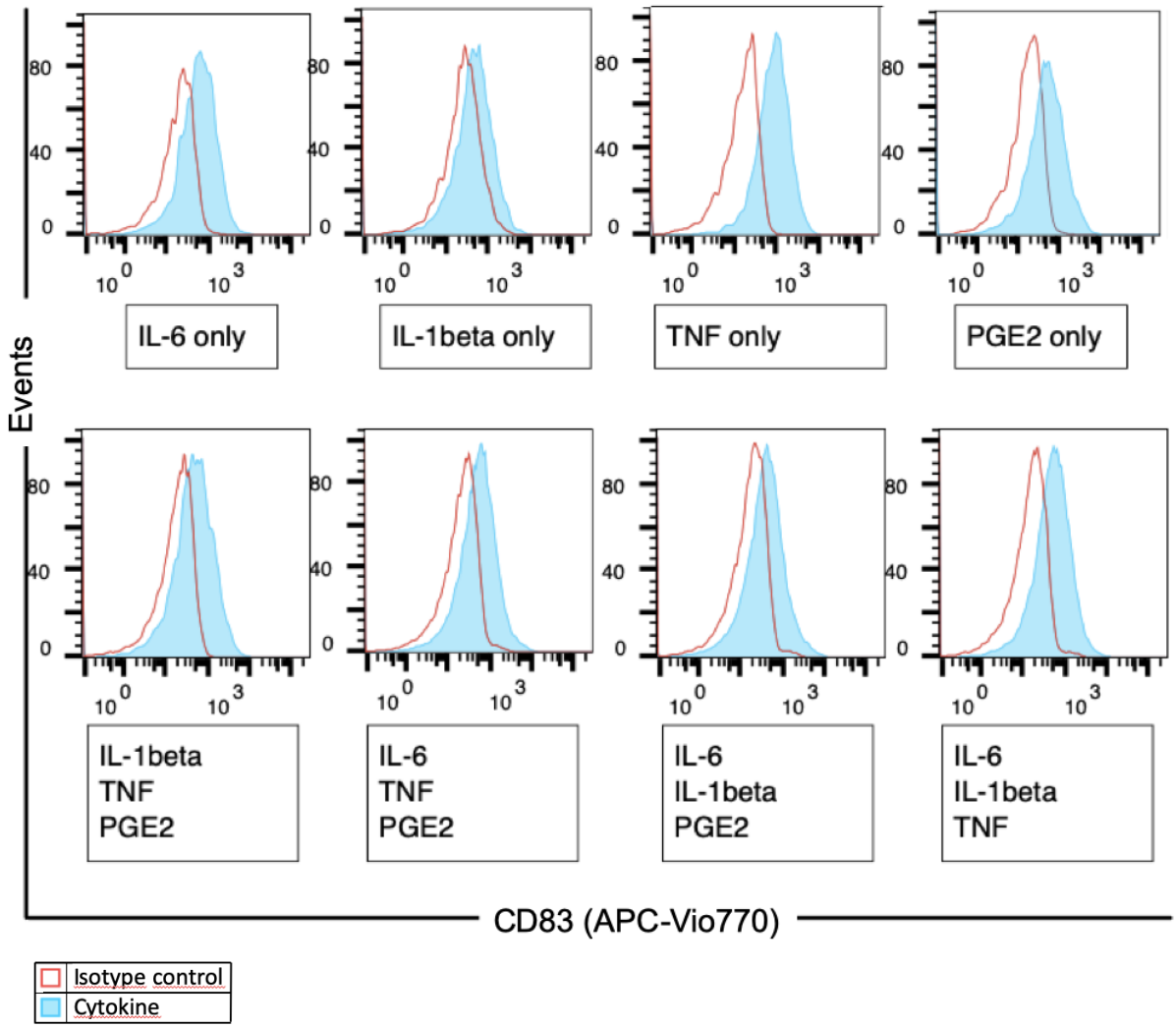

Figure 5 - FACS analysis demonstrating the results of experiments evaluating CD83 cell surface expression after addition of only one cytokine of the maturation cocktail (upper row) and addition of three out of four cytokines of the maturation cocktail (lower row). A673 cells were stained for CD83 using CD83 APC-Vio770-labelled antibodies (blue histogram). APC-Vio770 isotype-labelled control samples were generated for each cytokine or cytokine group individually (red histogram). This figure demonstrates the extent of increase of CD83 cell surface expression.

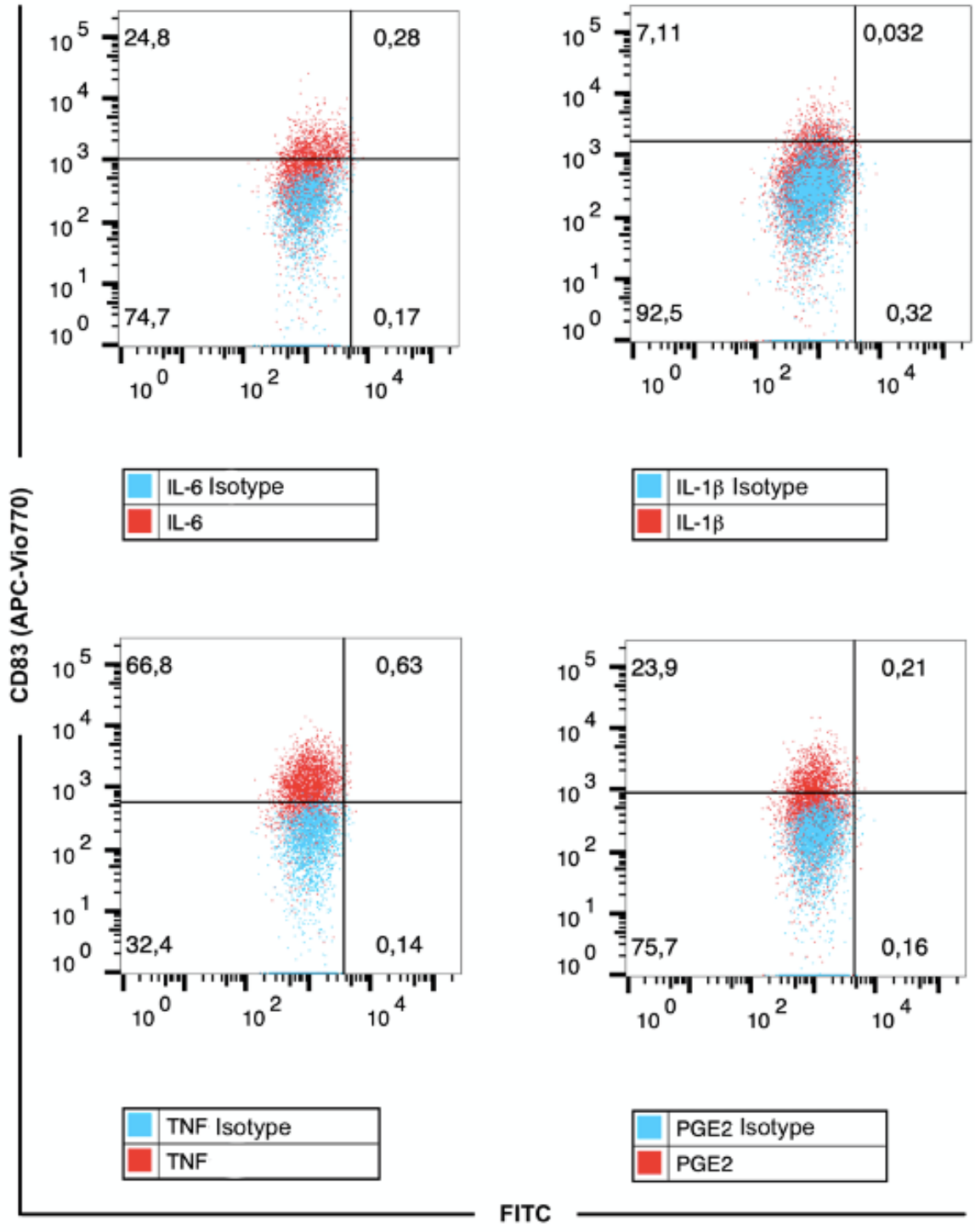

Figure 6 - FACS analysis demonstrating CD83 upregulation by addition of only one cytokine of the maturation cocktail. This graph only shows A673 cells stained for CD83 using CD83 APC-Vio770 labelled antibodies (red). Gates were set according to A673 cells stained with APC-Vio770 labelled isotype controls (blue).

Evaluating increased effect with increased dose of cytokines

Comparison of CD83 expression of tumor cells treated with single dose of cytokines with treatment of five-fold dose of cytokines yielded no distinct difference (see **Figure 7**).

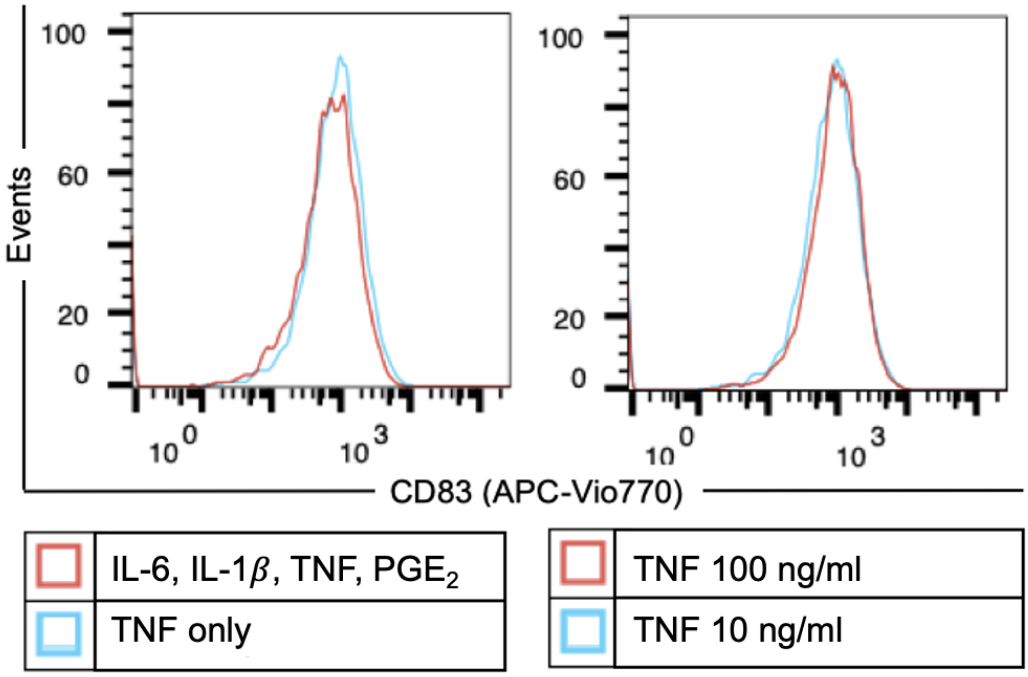

Figure 7 - FLOW cytometry analysis demonstrating the extent of difference of increase in CD83 cell surface expression between A673 cells matured in the full maturation cocktail (red histogram) and TNF only (blue histogram) as well as the difference between A673 cells cultivated in five-fold dose TNF (red histogram) compared to single dose TNF (blue histogram) (left graph). A673 cells were stained for CD83 using CD83 APC-Vio770-labelled antibodies.

Identification of point of time

In an attempt to assess the exact point of time of CD83 upregulation, we performed FACS analysis of day four (d4), day six (d6) and day seven (d7) of the dendritic cell medium protocol. On d4 and d6, no upregulation of CD83 could be identified. On d7, FACS analysis demonstrated a CD83 upregulation as seen in previous experiments (data not shown).

T cell mediated recognition and killing

The correlation between CD83 upregulation and T cell mediated recognition and killing of EwS tumor cells was demonstrated by ELISpot assay and Granzyme B assay, respectively. As the A673 cell line is HLA-A*02:01$^+$ whereas SBSR-AKS is an HLA-

A*02:01^{-} cell line, experiments were conducted with A673 only comparing A673 supplemented groups and A673 control groups.

ELISpot Assay

For the ELISpot assay, T2 cells pulsed with Influenza and CHM1-Peptides served as negative and positive control groups, respectively. CHM1^{319} specific TCR-transgenic T cells used were generated by our research group previously and were thawed and expanded by adding 100 U/ml recombinant human interleukin 2 (rhIL-2) and 2 ng/ml recombinant human interleukin 15 (rhIL-15). For the ELISpot assay, we assessed T cell recognition using two different effector to target ratios (10000:20000 and 5000:20000) to illustrate the effect in more detail. As shown in **Figure 8**, A673 cells cultivated in dendritic cell medium showed a significant increase in T cell recognition as indicated by IFNγ spots. Standard deviation and p-values are displayed in **Figure 8.**

Granzyme B Assay

For the ELISpot assay, T2 cells pulsed with Influenza and CHM1-Peptides served as negative and positive control groups, respectively, and CHM1^{319} specific TCR-transgenic T cells previously generated were used. Overall, the Granyzme B assay demonstrated improved T cell mediated killing of A673 tumor cells when cultivated in dendritic cell medium compared in all effector to target titrations. Standard deviations and p-values are displayed in **Figure 8.** In particular, it was observed that lower effector to target ratios yielded a bigger effect on T cell mediated killing indicating a more relevant effect at lower ratios.

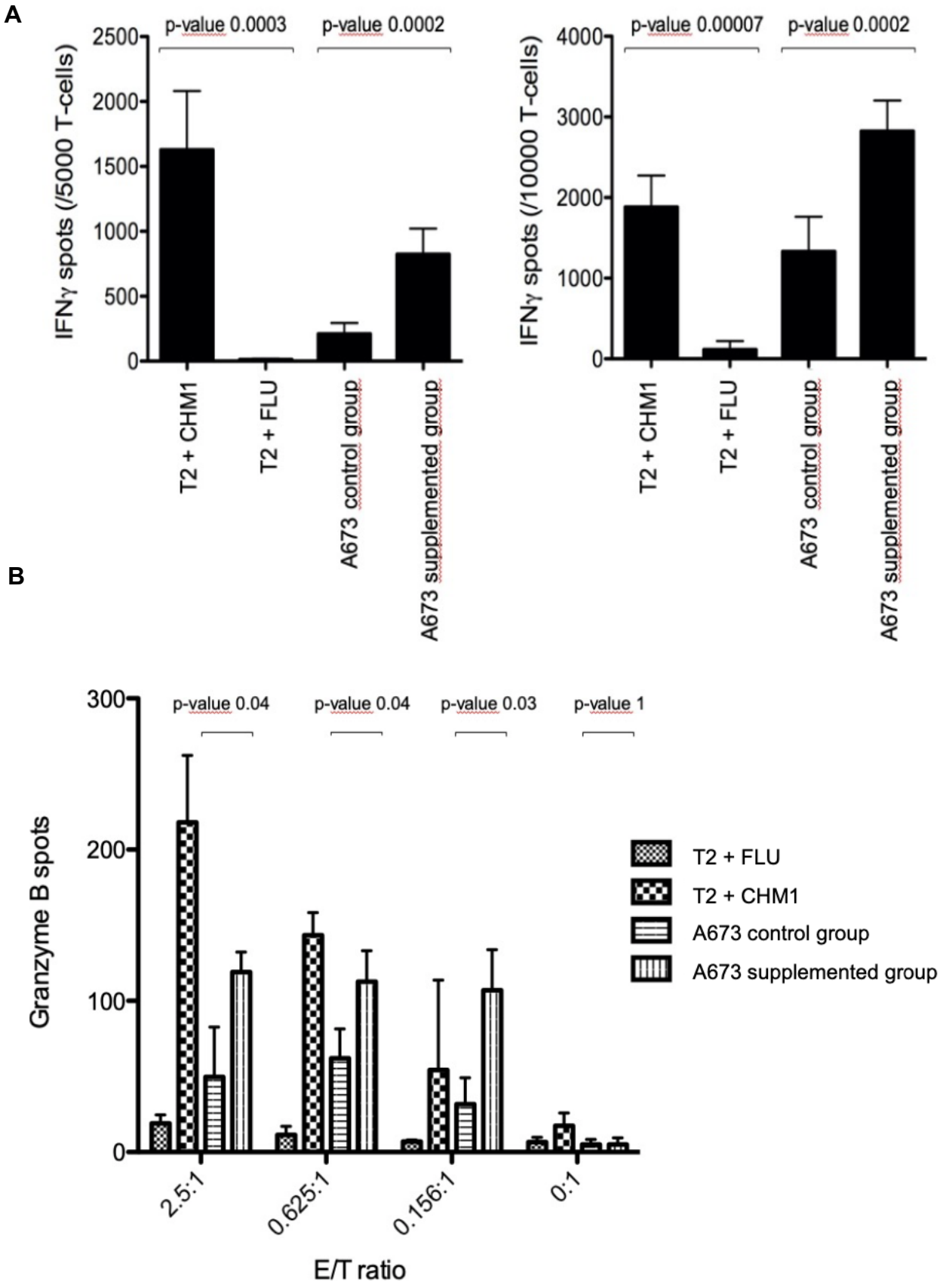
A
p-value 0.0003
p-value 0.0002
IFNγ spots (/5000 T-cells)
2500
2000
1500
1000
500
0
T2 + CHM1
T2 + FLU
A673 control group
A673 supplemented group
p-value 0.00007
p-value 0.0002
IFNγ spots (/10000 T-cells)
4000
3000
2000
1000
0
T2 + CHM1
T2 + FLU
A673 control group
A673 supplemented group
B
p-value 0.04
p-value 0.04
p-value 0.03
p-value 1
Granzyme B spots
300
200
100
0
2.5:1
0.625:1
0.156:1
0:1
E/T ratio
T2 + FLU
T2 + CHM1
A673 control group
A673 supplemented group

Figure 8 - $CHM1^{319}$/HLA-A*02:01-specific T cell mediated recognition and killing of A673 EwS cell lines and T2 pulsed cells in interferon-γ and granzyme B ELISpot assays. Error bars indicate standard deviation of sextuplicates. **A)** Interferon-γ ELISpot assays; A673 and $CHM1^{319}$ peptide-loaded T2 cells are specifically recognized by $CHM1^{319}$/HLA-A*02:01-specific T cells as compared to T2 cells loaded with influenza-derived control peptides. A673 supplemented with DC maturation cytokines, induce a significantly higher interferon-γ secretion as compared to non-supplemented A673 when 5.000 or 10.000 effector cells were used, respectively (both $p<0.05$). **B)** Granzyme B ELISpot assay; Dose dependent $CHM1^{319}$/HLA-A*02:01-specific T cell mediated killing of A673 and T2 cells loaded with $CHM1^{319}$ compared to influenza control peptide loaded T2 cells (FLU). A673 supplemented with DC maturation cytokines induce a significantly higher granzyme B secretion compared to non-supplemented A673 in effector to target ratios of 2.5 ($p=0.04$), 0.625 ($p=0.04$) and 0.156 ($p=0.03$).

Methodological Difficulties

Despite successful conduction of all experiments stated above, certain experiments could not be performed as expected or yielded incongruent results.

As stated previously, the TC71 EwS cell line showed a considerable rate of detachment from the flask on day seven upon addition of the maturation cocktail on day six which was much more severe than seen in the other two cell lines. When counting the culture TC71 cells as described previously, very few to none viable cells were visible. Several alterations aiming for improved TC71 culturing and thawing were attempted. We cultivated both a higher and smaller amount of TC71 cells.

Furthermore, we decreased the time of cultivation with the maturation cocktail from 24 hours to 12 hours. However, none of these attempts improved the cell state upon addition of the maturation cocktail. Hence, after thorough discussion with multiple members of the research group, we rendered TC71 cells unsuitable for further experiments and introduced the cell line SBSR-AKS instead.

A further issue associated with flask adherence of tumor cells was encountered when attempting to perform a real time cell analysis (RTCA) assay, which mechanism mainly relies on adherence of cells [42]. It was discussed, whether results obtained by RTCA assay are indicative of improved T cell mediated killing, giving that a vast amount of tumor cells showed detachment upon addition of the maturation cocktail. Therefore, we decided to perform a Granzyme B assay, where T cell mediated killing is measured by secreted Granzyme B instead of dissociation of cell adhesion.

Finally, one the overall four performed ELISpot assays did not show appropriate results. Neither positive nor negative control lines showed an increase of IFNγ spots, indicating that the experiment was not conducted correctly. Whether this issue was due to false experiment performance or defective material, such as the ELISpot plates used, is unknown. However, further ELISpot assays performed after this assay using the exact same materials demonstrated sufficient results.

Discussion

Despite recent advances in treatment of oncological disease, the prognosis for EwS patients, especially with refractory disease or early metastatic spread, remains poor. The rapidly advancing treatment option of immunotherapy is a promising approach for many tumor entities, including EwS. Although yielding encouraging results in other paediatric malignancies, immunotherapy using adoptive T cell treatment has shown a diminished success rate in EwS. This may partly be attributed to low mutational burden as well as decreased numbers of TILs within tumoral tissues observed in EwS. However, despite generating heterogenous results, the use of autologous stem cell therapy in addition to chemotherapeutic agents has produced favourable outcomes as presented in in recent studies and hence implied that further investigations may yield promising results [16, 17]. Our research group has previously succeeded in generating CHM1-specific TCR-transgenic T cells that showed initial anti-tumoral effects in vitro and in vivo. In this work, we sought to render immunologically cold EwS more susceptible to T cell mediated immunotherapy by altering the tumor microenvironment to a more inflammatory-prone state.

Human CHM1 is a transmembrane glycoprotein first described by Hiraki et al. and is mainly found in immature and avascular cartilage. CHM1 is known to be a key regulator of angiogenesis during chondrocyte differentiation in endochondral bone development [44, 45]. Since its discovery, the role of CHM1 in disease progression such as osteoarthritis, but also pediatric cancers such as osteosarcoma and EwS, has been established [62, 110]. Although a surprising finding in malignancies, it has become evident that the anti-angiogenic properties of CHM1 result in hypoxic tumor tissue and are therefore associated with a more aggressive tumor nature and increased risk of metastasis [27, 94]. Our research group has demonstrated the direct link and resulting upregulation between the fusion oncogene EWS-FLI1 and CHM1, which is likely to lead to the significant overexpression of CHM1 observed in EwS. Through various experiments, we were able to identify CHM1 as a responsible agent enhancing malignant potential as well as the capacity of metastatic spread in EwS [103]. Taken together, CHM1 posed an ideal target for TCR therapy as it has shown to be overexpressed on EwS cells in correlation to the expression of EWS-FLI1 oncogene, which occurs in 85% of EwS cases, without being expressed in normal tissues, as well as being an important driver of tumor sustainment and metastatic spread.

In following experiments, our research group has successfully generated HLA-A*02:01-restricted peptide-specific CHM1^{319} cytotoxic T cells by priming naïve T cells using HLA-A02:01^{+} dendritic cells pulsed with CHM1-peptides. These experiments have yielded encouraging results by demonstrating peptide-specificity as well as responsiveness of EwS cells in mouse models [94]. When performing this experiment in an autologous setting, the generated T cells were unable to recognize and kill EwS cells hence rendering them less suitable for further experiments. Despite initial successes of this treatment approach, the complex generation yielding only low numbers of T cells that were quickly exhausted upon initial action rendered the incorporation of this approach into therapy protocols unrealistic. Hence, our research group generated HLA-A*02:01-restricted peptide-specific CHM1^{319} cytotoxic T cells by retroviral transduction resulting in transgenic T cells [10]. In vivo and in vitro studies using the generated T cells have further demonstrated satisfactory T cell recognition and killing of EwS cell lines. In 2017, Thiel et al. first administered the generated T cells to three refractory EwS patients and demonstrated encouraging results. After assessment of CHM1 expression on EwS tissues of the patients and establishing in vitro lysis of EwS cell lines by generated T-cells, HLA-A*02:01/CHM1^{319} -specific allorestricted CD8^{+} T cells were administered. Overall, the administration of T cells demonstrated slow disease progression in two patients and homing of the T cells to tumor sites yielding a partial metastatic regression of EwS in one patient without causing any signs and symptoms of graft versus host disease which suggests peptide-specificity [95]. Also of note is the persistence of CHM1 transgenic T cells in the bone marrow for weeks after transfusion. Despite demonstrating partial tumor regression, all three patients, who presented with highly advanced tumors at the time of T cell administration, died within two to five months following the transfer of T-cells. However, a matched pair analysis, despite low number of patients, showed an increased mean overall survival in patients receiving adoptive T cell therapy as compared to a control group of the EURO-Ewing 2008 treatment regime [95]. These findings demonstrated the efficacy of HLA-A*02:01/CHM1^{319} -specific allorestricted CD8^{+} T cells in advanced EwS without causing adverse GvHD and thereby opened access to a novel therapeutic approach.

The aim of this thesis was to further enhance the efficacy of the EwS antigen-specific T cells generated by our research group by upregulating the surface marker CD83 on EwS cell lines.

Phenotype of EwS tumor cells lines matured in dendritic cell medium

As illustrated by our results, the EwS tumor cell lines A673 and SBSR-AKS showed a distinct alteration of their phenotype in response to cultivation in medium conventionally used for the generation of mature dendritic cells.

One of the most interesting alteration was the observed upregulation of cell surface marker CD83, which is a key regulator of immune response and, in its membrane-bound form, is suggested to exert pro-inflammatory functions, mainly by T cell development and antagonizing MARCH-driven downregulation of surface markers involved in generating an immune response [33]. In the past, it has become apparent that CD83 is a key regulator of immune response, directing both pro-inflammatory signals as well as regulatory signals hampering overshooting immune responses. As described previously, the importance of CD83 in T cell generation, differentiation and activation as well as its stabilizing effect of important surface molecules has been thoroughly demonstrated throughout the past decades. Moreover, interesting findings have demonstrated the importance of CD83 on regulating the immune response. For one, investigations have demonstrated the adverse effect on exacerbation of colitis in $CD83^{-/-}$ mice [5]. Furthermore, overexpression of CD83 seems to be associated with inhibitory effects on B-cell function despite the observed increase in surface CD86 and MHC class II [57].

The distinct mechanism of action by which CD83 exerts its function is not entirely known. However, in the literature, it has been described that CD83 exerts various functions by antagonization of the ubiquitin ligase MARCH-1 and MARCH-8 [63, 99]. Although we did not evaluate surface expression of MARCH receptors, investigation of RNA did not show a trend in upregulation or downregulation of either ligands with EwS cell lines (data not shown). Although CD83, a specific marker for mature dendritic cells, was upregulated in our findings, we did not observe an upregulation of other markers for dendritic cells such as HLA-DR, CD80 or CD86. Hence, we conclude that EwS cell lines upregulate the expression of individual surface markers following the cultivation with the specific cytokines rather than undergoing differentiation.

Correlation between CD83 upregulation and improved T cell function

The upregulation of CD83 on cell surface and RNA level was correlated with and enhanced function of HLA-A*02:01-restricted peptide-specific CHM1^{319} cytotoxic T cells as demonstrated by increased recognition and killing of tumor cells (see results). Although we are not able to identify the exact mechanism underlying this correlation, two mechanisms pay pose potential explanations.

First, we observed an increase of MHC class I and II expression on EwS tumor cells cultivated in dendritic cell cell medium that was seemingly positively correlated to CD83 upregulation. As MHC class I and II are primarily involved in T cell activation by antigen presentation on cell surface and priming of CD8$^+$ T-cells, the upregulation may play a role in the enhanced tumor cell T cell interaction [30, 40]. As indicated previously, several types of cancers downregulate their cell surface MHC expression over time generating an 'escape mechanism' by which they dampen the immune response directed against tumor tissue [20, 35]. Experiments conducted by Berghuis et al. investigating the MHC class I and II expression on 67 EwS cell lines by flow cytometry and immunofluorescence staining have obtained heterogenous results. However, the research group found that the majority of EwS cell lines demonstrated a substantial downregulation of MHC class I expression on EwS cells, including metastatic tissues implying the negative effect it bears on immunotherapy[7, 68]. Further studies conducted by Yabe et al. demonstrated a decreased infiltration of CD8$^+$ T cells in response to MHC class I downregulation which in turn resulted in a significantly poorer overall survival[106]. Hence, the upregulated MHC expression observed in our results may be an attempted reverse of that particular escape mechanism, although in order to confirm this hypothesis, further investigations are required. It has to be critically assessed, however, that prior to both ELISpot and Granzyme B assay, IFNγ was added to the target cells according to the protocols. In the literature, IFNγ is described to upregulate and stabilize the MHC class I surface expression by inducing genes that are related to MHC class I expression and its functions as an antigen presenting agent [102, 107]. Therefore, one may argue that the increase in surface MHC expression and the correlated enhanced T cell activation is caused by addition of IFNγ rather than the dendritic cell medium. However, we observed an upregulated MHC expression by FACS analysis and also microarray analysis, where tumor cells have never been treated with IFNγ. Hence, we conclude that the increase in MHC in our experiments are not driven by the addition of IFNγ. Overall, further experiments are required to test

these hypotheses, in particular selective MHC blockage to assess whether MHC expression is responsible for enhanced T cell activation or if other underlying mechanisms are of higher relevance.

A second mechanism which may positively influence T cell function in the observed co-expression and upregulation of CD83 and intracellular adhesion molecule-1 (ICAM-1). ICAM-1, also known as CD54, is a transmembrane glycoprotein of the Ig superfamily and is mostly known due to its co-stimulatory function enhancing the interaction between dendritic cells and T cells [92]. Upon cell activation by inflammatory mediators, constantly expressed ICAM-1 is upregulated through increased gene transcription[77]. ICAM-1 is commonly expressed on cells involved in the immune response although expression on tumor cell surface has been demonstrated. Investigation by Bailey et al. have demonstrated that ICAM-1 is able to promote T cell activation and T-cell/tumor cell interaction by highly specific binding of ICAM-1 expressed on tumor cells and the corresponding lymphocyte function associated antigen-1 (LFA-1 or CD11a) expressed on lymphocytes [2, 77]. Hence, ICAM-1 expression on tumor cells poses an option of enhanced T cell activation and favorable outcome which could be observed in colorectal cancer, where a correlation between ICAM-1 expression and improved prognosis was established[65, 75]. As ICAM-1 has shown to be effective in improving T-cell/tumor cell interaction in EwS, this might be a potential mechanism underlying the improved T cell mediated recognition and killing that we observed in our findings. In their research, Bailey et al. have established that ICAM-1 expression is induced by IFNγ, however, as our experiments did not involve treatment of tumor cells with IFNγ, another underlying mechanism is responsible, which has not been further explored in this work [2].

Expression of PD-L1

The programmed cell death-1 (PD-1) pathway is checkpoint pathway that has shown to be an established target in immunotherapy. PD-1 is a regulatory agent and is most significantly known for its inhibitory effect on T cell activation. Although mostly expressed on cells involved in immune responses, the corresponding ligand, PD-L1, can be expressed by tumor cells where it has shown to have an immune-evading effect diminishing immunological efficacy directed against tumor cells [86, 109]. Hence, immune checkpoint inhibitors directed against PD-1 or PD-L1 and thereby reversing

the T cell tolerance have been generated and showed significant results in various cancer types such as melanoma or non-small-cell lung cancer [93]. However, the efficacy of PD-L1 checkpoint inhibitors as demonstrated in various cancer entities was not as encouraging in EwS patients. A phase two clinical trial treating patients with advanced soft-tissue or bone sarcoma with the PD-1 checkpoint inhibitor pembrolizumab demonstrated no response towards treatment [93]. This diminished efficacy is mainly attributed to the absent or low expression of PD-L1 by EwS tumor cells as well as the TME [68, 89, 101].

TNF as most potent cytokine driving CD83 upregulation

The exact mechanism of CD83 processing and cell surface expression is not entirely understood. It has been suggested that CD83 expression on T-lymphocytes is regulated via the transcription factor NFκB [67]. Further evidence suggests that in immature dendritic cells, CD83 is preformed intracellularly and is rapidly expressed on cell surface upon activation and maturation [18, 39]. In our experiments, we demonstrated upregulation of CD83 among other cell surface proteins by cultivation of tumor cells in presence of cytokines conventionally used in generation of mature dendritic cells. Although expression of CD83 on cells involved in immune response has been described extensively, to our knowledge CD83 expression on tumor cells and its role in the induction of anti-tumor responses is not considerably distinguished in the literature. We were not able to identify one single cytokine responsible for the CD83 upregulation as all cytokines demonstrated CD83 upregulation when used individually. Nonetheless, TNF demonstrated the most considerable CD83 upregulation and may therefore be suggested as the most potent cytokine driver. These findings are in line with previous reports identifying TNF as an activating agent for increased CD83 expression on monocyte derived dendritic cells and therefore a potent driver for dendritic cell maturation [72, 80].

TNF, initially identified in the 1970s, is an inflammatory cytokine that is secreted by macrophages, monocytes, and T-lymphocytes upon activation and exerts mainly pro-inflammatory actions [19]. The biological functions of TNF mainly concern activation and stimulation of immune cells and thrombocytes to enhance immune response upon pathogen encounter [49]. Given these functions, the application of monoclonal antibodies directed against TNF, such as infliximab, have revolutionized the treatment of disease with overshooting inflammatory responses such as inflammatory bowel

disease or ulcerative colitis [70]. The biological effects of TNF on tumor cells have also been investigated. It has been described in the literature that in about a third of tumors soluble TNF yields cell death by mechanisms including increased cellular apoptosis, antagonizing Treg action with correlated enhanced T cell activation or destruction of tumor microvasculature or promotion of M1 macrophages [48, 51, 69]. Despite these anti-tumor properties, investigation have also demonstrated that TNF, if dysregulated, is able to mediate effects that favor progression of malignancy [85]. Reversely, tumor cells are able to secrete TNF which then acts as an autocrine growth factor inducing tumor cell proliferation [85].

The use of TNF as an anti-tumor agent has yielded heterogenous results in the past. On one hand, simultaneous application of TNF and other anti-cancer agents resulted in an increased uptake and enhanced efficacy of anti-tumor agents. On the other hand, TNF has shown to induce severe toxicity at doses even lower than the predicted efficient dose [24, 88]. Despite the limitations of use, investigations conducted by Lienard et al. in 1992 demonstrated that local administration of TNF, IFNγ and melphalan by isolated limb perfusion in melanoma and soft tissue sarcoma patients demonstrated successful disease regression via destruction of tumor micro vascularization with acceptable toxicity rates [61]. Despite the successful treatment, patients had to receive prophylactic dopamine and hyperhydration treatment in order to minimize toxic effects.

In the literature, there are several mechanisms described which result in an upregulation of peripheral TNF levels by induction of inflammation in EwS cell lines. Multiple research groups have observed an upregulation of TNF mRNA and protein levels in response to irradiation in a time-dependent manner in TNF producing EwS cell lines [21, 81, 100]. In addition, irradiation or hyperthermia has shown to lead to an increase in TNF transcription without causing any remarkable side-effects [11, 74].

Taking these previous findings together, the incorporation of TNF into current immunotherapeutic treatment regimens such as treatment with CHM1^{319} specific TCR-transgenic T cells might render EwS tumor cells more susceptible for T cells recognition and killing via inducing a CD83 upregulation. As there are several mechanisms to induce TNF secretion via the induction of local inflammation in vivo, this finding may offer a new therapeutic approach to improve conditioning regimes, especially for adoptive T cell based immunotherapy.

Summary

Paediatric EwS is a tumor of bone and soft tissue that is characterized by the distinct genetic signature of EWS-ETS family fusion oncogene. Despite significant improvement of therapeutic approaches targeting EwS, immunotherapy has not yet yielded as encouraging results as it has in other tumor entities. It has become apparent that EwS harbours a low somatic mutational burden as well as small numbers of tumor infiltrating T cells hence suggesting a relatively low immunogenicity. Our research group has pursued the improvement of adoptive T cell therapy in EwS by successfully generating tumor antigen specific transgenic T-cells, that have demonstrated efficacy in vitro and in vivo. The aim of this thesis was to further enhance HLA-A*02:01/CHM1^{319} -specific allorestricted CD8^{+} T cell function by increasing the cell surface expression of CD83, a glycoprotein most commonly known as a highly specific marker for mature dendritic cells. CD83, in its membrane-bound form, has shown to play a key regulatory role in generating an immune response. Specifically, CD83 has demonstrated its important function in T cell differentiation and activation as well as stabilization of surface markers on B-cells and dendritic cells.

In this work, we demonstrated the reciprocal induction of upregulation of CD83 on cell surface and RNA level. Furthermore, we were able to identify a positively correlated upregulation of important surface markers involved in immune responses such as MHC class I and ICAM-1. Interestingly, the upregulation of said surface markers was in turn correlated with an improved recognition and killing of tumor cells mediated by HLA-A*02:01/CHM1^{319} -specific allorestricted CD8^{+} T-cells, which may suggest an enhanced T cell efficacy in vivo. Although the exact mechanisms of CD83 upregulation remain to be investigated, we were able to identify TNF to be the most potent cytokine that drives CD83 upregulation when used as a single agent, although all other cytokines of the maturation cocktail were able to induce an upregulation when used alone, but to a lesser extent.

In conclusion, this work has demonstrated that EwS tumor cells can be altered to become more susceptible to the effect of adoptive T cell therapy by manipulation of the tumor microenvironment in vitro. In the future, further investigations should be conducted to evaluate whether these changes can also be seen in vivo which in turn may suggest the incorporation of novel agents such TNF into existing treatment regimes.

Appendix

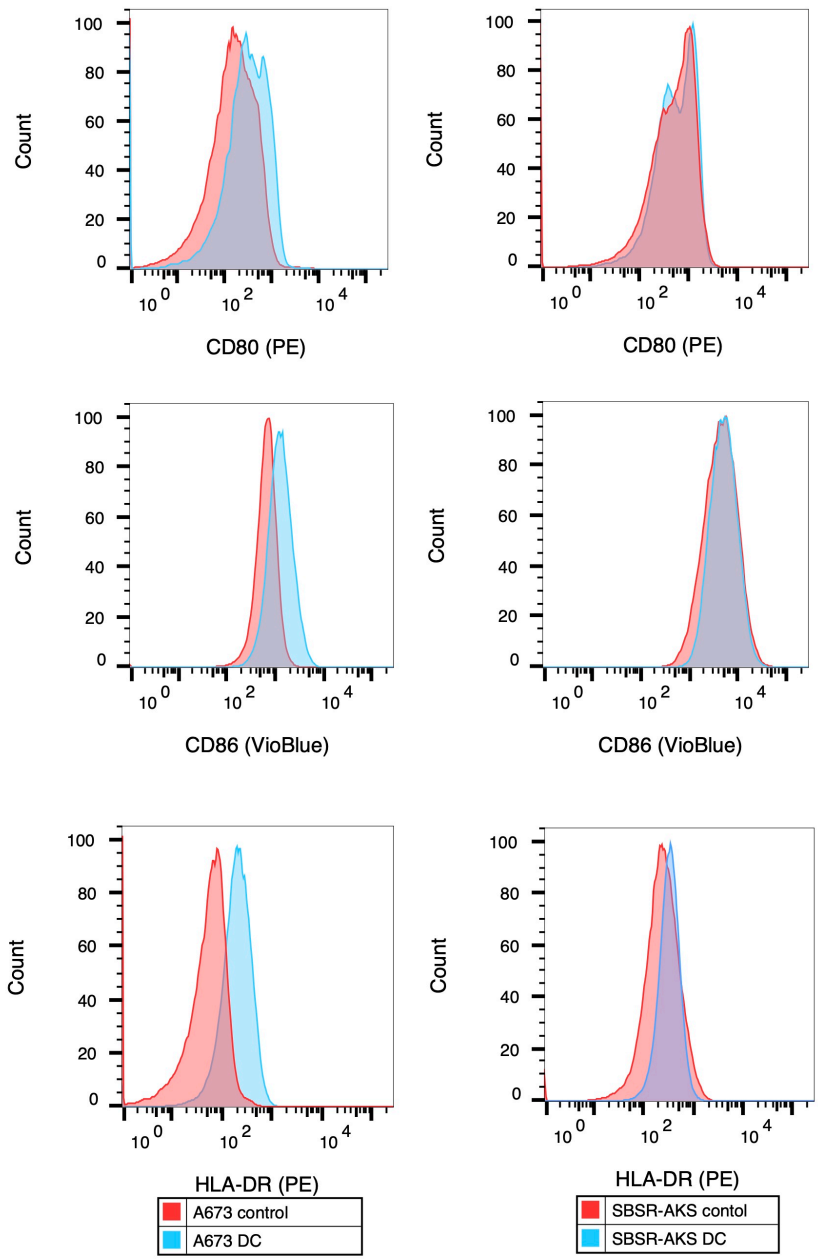

Appendix 1 – Flow Cytometry Data displaying markers of mature dendritic cells CD80, CD86 and HLA-DR. Gates were set according to isotype control-labelled antibodies. As demonstrated, there was no distinct upregulation observed in either of the surface markers in either A673 nor SBSR-AKS cell line.

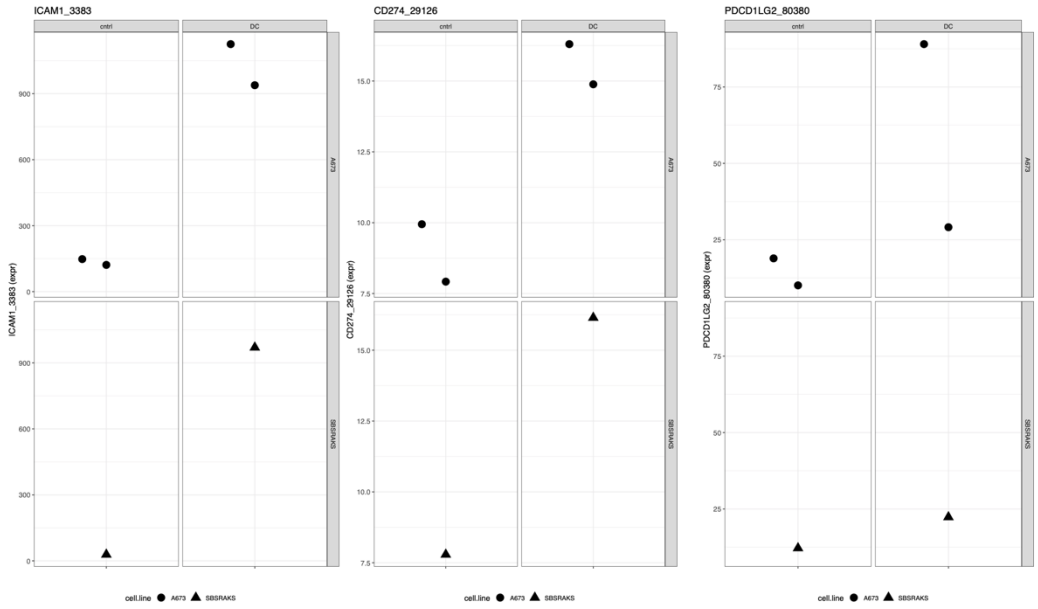

FeatureAssay Plot - ICAM FeatureAssay Plot - PD-L1 FeatureAssay Plot - PD-L2

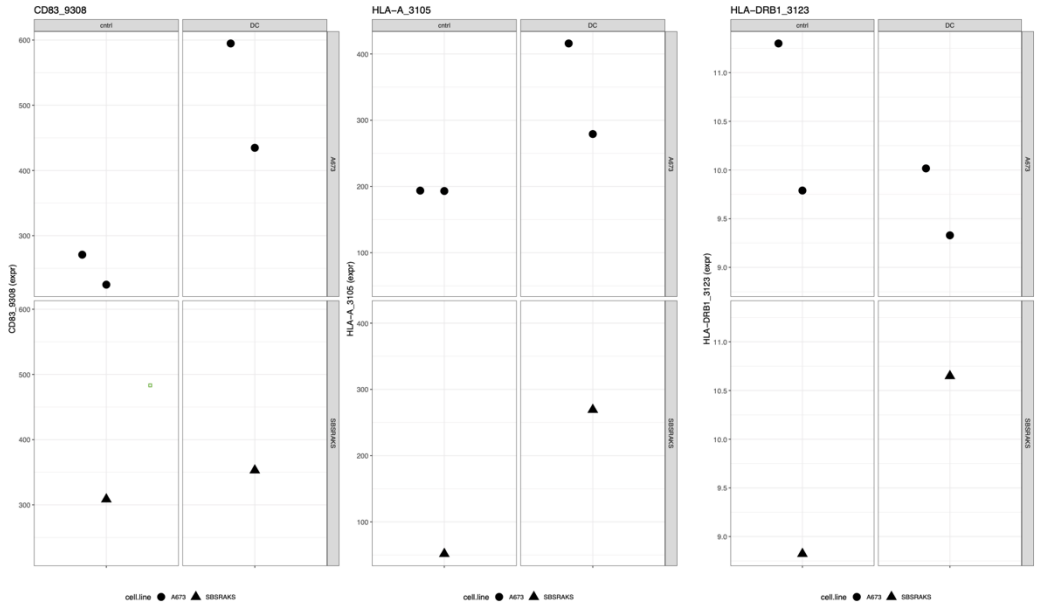

FeatureAssay Plot - CD83 FeatureAssay Plot - MHC I FeatureAssay Plot - MHC II

Appendix 2 – FeatureAssay Plots generated with iSEE software. The plots demonstrate the changes of mediator involved in an immune response on RNA level observed in control groups (cntrl / left hand columns) and supplemented groups (dendritic cells / right hand columns).

Acknowledgements

First and foremost, I would like to thank PD Dr. Uwe Thiel and Prof. Dr. Stefan Burdach for giving me the opportunity to conclude my research project in the Laboratory 'Labor für krebskranke Kinder' as part of an established team of researchers.

During the time of my research, I received an enormous amount of support by all members of the team.

Thank you to PD Dr. Uwe Thiel for being a constant source support, both emotional and in terms of scientific expertise, as well as providing excellent supervision and mentorship. I would like to thank Dr. Sebastian Schober, Dr. Hendrik Gaßmann, and Dr. Kristina von Heyking for their support, invaluable council, and patience throughout the project. Furthermore, thank you Melanie Thiede, Carolin Prexler and Corazón Kordass for teaching me my laboratory skills, answering all my questions and tirelessly supporting me and my work.

I sincerely thank all other members of the laboratory team who have made working a memorable, enlightening and enjoyable experience.

It goes without saying that I highly appreciate all the support I have received as well as all the things I have learned throughout the past months. I consider myself very lucky to have had such a positive insight into the field of scientific medicine and will cherish that experience throughout the rest of my personal and professional life.

Last but not least, thank you to my two most valuable emotional supporters, Elena for constantly listening to my worries and setbacks, caring for me in times of need and giving me energy to keep on going and of course, Katharina Lutz for being the best companion throughout these exciting times anyone could have asked for.

References

[1] P. J. Amrolia, S. D. Reid, L. Gao, B. Schultheis, G. Dotti, M. K. Brenner, J. V. Melo, J. M. Goldman, and H. J. Stauss, "Allorestricted cytotoxic T cells specific for human CD45 show potent antileukemic activity," *Blood,* vol. 101, no. 3, pp. 1007-14, Feb 1 2003, doi: 10.1182/blood-2002-02-0525.

[2] K. M. Bailey, C. M. Julian, A. N. Klinghoffer, H. Bernard, P. C. Lucas, and L. M. McAllister-Lucas, "EWS-FLI1 low Ewing sarcoma cells demonstrate decreased susceptibility to T-cell-mediated tumor cell apoptosis," *Oncotarget,* vol. 10, no. 36, pp. 3385-3399, May 21 2019, doi: 10.18632/oncotarget.26939.

[3] M. C. Baldauf, M. F. Orth, M. Dallmayer, A. Marchetto, J. S. Gerke, R. A. Rubio, M. M. Kiran, J. Musa, M. M. L. Knott, S. Ohmura, J. Li, N. Akpolat, A. N. Akatli, O. Ozen, U. Dirksen, W. Hartmann, E. de Alava, D. Baumhoer, G. Sannino, T. Kirchner, and T. G. P. Grunewald, "Robust diagnosis of Ewing sarcoma by immunohistochemical detection of super-enhancer-driven EWSR1-ETS targets," *Oncotarget,* vol. 9, no. 2, pp. 1587-1601, Jan 5 2018, doi: 10.18632/oncotarget.20098.

[4] D. W. Barnes, M. J. Corp, J. F. Loutit, and F. E. Neal, "Treatment of murine leukaemia with X rays and homologous bone marrow; preliminary communication," *Br Med J,* vol. 2, no. 4993, pp. 626-7, Sep 15 1956, doi: 10.1136/bmj.2.4993.626.

[5] J. M. Bates, K. Flanagan, L. Mo, N. Ota, J. Ding, S. Ho, S. Liu, M. Roose-Girma, S. Warming, and L. Diehl, "Dendritic cell CD83 homotypic interactions regulate inflammation and promote mucosal homeostasis," *Mucosal Immunol,* vol. 8, no. 2, pp. 414-28, Mar 2015, doi: 10.1038/mi.2014.79.

[6] D. Berghuis, S. J. Santos, H. J. Baelde, A. H. Taminiau, R. M. Egeler, M. W. Schilham, P. C. Hogendoorn, and A. C. Lankester, "Pro-inflammatory chemokine-chemokine receptor interactions within the Ewing sarcoma microenvironment determine CD8(+) T-lymphocyte infiltration and affect tumour progression," *J Pathol,* vol. 223, no. 3, pp. 347-57, Feb 2011, doi: 10.1002/path.2819.

[7] D. Berghuis, A. S. de Hooge, S. J. Santos, D. Horst, E. J. Wiertz, M. C. van Eggermond, P. J. van den Elsen, A. H. Taminiau, L. Ottaviano, K. L. Schaefer, U. Dirksen, E. Hooijberg, A. Mulder, C. J. Melief, R. M. Egeler, M. W. Schilham, E. S. Jordanova, P. C. Hogendoorn, and A. C. Lankester, "Reduced human leukocyte antigen expression in advanced-stage Ewing sarcoma: implications for immune recognition," *J Pathol,* vol. 218, no. 2, pp. 222-31, Jun 2009, doi: 10.1002/path.2537.

[8] M. Bernstein, H. Kovar, M. Paulussen, R. L. Randall, A. Schuck, L. A. Teot, and H. Juergens, "Ewing's sarcoma family of tumors: current management," *Oncologist,* vol. 11, no. 5, pp. 503-19, May 2006, doi: 10.1634/theoncologist.11-5-503.

[9] R. E. Billingham, L. Brent, and P. B. Medawar, "Quantitative studies on tissue transplantation immunity. II. The origin, strength and duration of actively and adoptively acquired immunity," *Proc. R. Soc. Lond. B. Biol. Sci.,* vol. 143, no. 910, pp. 58-80, Dec 15 1954, doi: 10.1098/rspb.1954.0054.

[10] F. Blaeschke, U. Thiel, A. Kirschner, M. Thiede, R. A. Rubio, D. Schirmer, T. Kirchner, G. H. S. Richter, S. Mall, R. Klar, S. Riddell, D. H. Busch, A. Krackhardt, T. G. Grunewald, and S. Burdach, "Human HLA-A*02:01/CHM1+ allo-restricted T cell receptor transgenic CD8+ T cells specifically inhibit Ewing sarcoma growth in vitro and in vivo," *Oncotarget,* vol. 7, no. 28, pp. 43267-43280, Jul 12 2016, doi: 10.18632/oncotarget.9218.

[11] M. N. Bouchlaka, D. Redelman, and W. J. Murphy, "Immunotherapy following hematopoietic stem cell transplantation: potential for synergistic effects," *Immunotherapy,* vol. 2, no. 3, pp. 399-418, May 2010, doi: 10.2217/imt.10.20.

[12] M. Breloer and B. Fleischer, "CD83 regulates lymphocyte maturation, activation and homeostasis," *Trends Immunol,* vol. 29, no. 4, pp. 186-94, Apr 2008, doi: 10.1016/j.it.2008.01.009.

[13] S. A. Burchill, "Ewing's sarcoma: diagnostic, prognostic, and therapeutic implications of molecular abnormalities," *J Clin Pathol,* vol. 56, no. 2, pp. 96-102, Feb 2003, doi: 10.1136/jcp.56.2.96.

[14] S. Burdach, U. Thiel, M. Schoniger, R. Haase, A. Wawer, M. Nathrath, H. Kabisch, C. Urban, H. J. Laws, U. Dirksen, M. Steinborn, J. Dunst, H. Jurgens, and E. S. G. Meta, "Total body MRI-governed involved compartment irradiation combined with high-dose chemotherapy and stem cell rescue improves long-term survival in Ewing tumor patients with multiple primary bone metastases," *Bone Marrow Transplant,* vol. 45, no. 3, pp. 483-9, Mar 2010, doi: 10.1038/bmt.2009.184.

[15] S. Burdach, B. van Kaick, H. J. Laws, S. Ahrens, R. Haase, D. Korholz, H. Pape, J. Dunst, T. Kahn, R. Willers, B. Engel, U. Dirksen, C. Kramm, W. Nurnberger, A. Heyll, R. Ladenstein, H. Gadner, H. Jurgens, and U. Go el, "Allogeneic and autologous stem-cell transplantation in advanced Ewing tumors. An update after long-term follow-up from two centers of the European Intergroup study EICESS. Stem-Cell Transplant Programs at Dusseldorf University Medical Center, Germany and St. Anna Kinderspital, Vienna, Austria," *Ann Oncol,* vol. 11, no. 11, pp. 1451-62, Nov 2000, doi: 10.1023/a:1026539908115.

[16] S. Burdach, H. Jurgens, C. Peters, W. Nurnberger, C. Mauz-Korholz, D. Korholz, M. Paulussen, H. Pape, D. Dilloo, E. Koscielniak, and et al., "Myeloablative radiochemotherapy and hematopoietic stem-cell rescue in poor-prognosis Ewing's sarcoma," *J Clin Oncol,* vol. 11, no. 8, pp. 1482-8, Aug 1993, doi: 10.1200/JCO.1993.11.8.1482.

[17] S. Burdach, "Treatment of advanced Ewing tumors by combined radiochemotherapy and engineered cellular transplants," *Pediatr Transplant,* vol. 8 Suppl 5, pp. 67-82, Jun 2004, doi: 10.1111/j.1398-2265.2004.00186.x.

[18] W. Cao, S. H. Lee, and J. Lu, "CD83 is preformed inside monocytes, macrophages and dendritic cells, but it is only stably expressed on activated dendritic cells," *Biochem J,* vol. 385, no. Pt 1, pp. 85-93, Jan 1 2005, doi: 10.1042/BJ20040741.

[19] E. A. Carswell, L. J. Old, R. L. Kassel, S. Green, N. Fiore, and B. Williamson, "An endotoxin-induced serum factor that causes necrosis of tumors," *Proc. Natl. Acad. Sci. U. S. A.,* vol. 72, no. 9, pp. 3666-70, Sep 1975, doi: 10.1073/pnas.72.9.3666.

[20] C. C. Chang and S. Ferrone, "Immune selective pressure and HLA class I antigen defects in malignant lesions," *Cancer Immunol Immunother,* vol. 56, no. 2, pp. 227-36, Feb 2007, doi: 10.1007/s00262-006-0183-1.

[21] L. Chang, Z. Zhang, F. Chen, W. Zhang, S. Song, and S. Song, "Irradiation enhances dendritic cell potential antitumor activity by inducing tumor cell expressing TNF-alpha," *Med Oncol,* vol. 34, no. 3, p. 44, Mar 2017, doi: 10.1007/s12032-016-0864-3.

[22] L. Chen, S. Guan, Q. Zhou, S. Sheng, F. Zhong, and Q. Wang, "Continuous expression of CD83 on activated human CD4(+) T cells is correlated with their differentiation into induced regulatory T cells," *Mol Med Rep,* vol. 12, no. 3, pp. 3309-3314, Sep 2015, doi: 10.3892/mmr.2015.3796.

[23] J. Couzin-Frankel, "Breakthrough of the year 2013. Cancer immunotherapy," *Science,* vol. 342, no. 6165, pp. 1432-3, Dec 20 2013, doi: 10.1126/science.342.6165.1432.

[24] P. J. Creaven, D. E. Brenner, J. W. Cowens, R. P. Huben, R. M. Wolf, H. Takita, S. G. Arbuck, M. S. Razack, and A. D. Proefrock, "A phase I clinical trial of recombinant human tumor necrosis factor given daily for five days," *Cancer Chemother Pharmacol,* vol. 23, no. 3, pp. 186-91, 1989, doi: 10.1007/BF00267953.

[25] U. Dirksen, B. Brennan, M. C. Le Deley, N. Cozic, H. van den Berg, V. Bhadri, B. Brichard, L. Claude, A. Craft, S. Amler, N. Gaspar, H. Gelderblom, R. Goldsby, R. Gorlick, H. E. Grier, J. M. Guinbretiere, P. Hauser, L. Hjorth, K. Janeway, H. Juergens, I. Judson, M. Krailo, J. Kruseova, T. Kuehne, R. Ladenstein, C. Lervat, S. L. Lessnick, I. Lewis, C. Linassier, P. Marec-Berard, N. Marina, B. Morland, H. Pacquement, M. Paulussen, R. L. Randall, A. Ranft, G. Le Teuff, K. Wheatley, J. Whelan, R. Womer, O. Oberlin, D. S. Hawkins, E. W. I. N. G. Euro, and I. Ewing, "High-Dose Chemotherapy Compared With Standard Chemotherapy and Lung Radiation in Ewing Sarcoma With Pulmonary Metastases: Results of the European Ewing Tumour Working Initiative of National Groups, 99 Trial and EWING 2008," *J Clin Oncol,* vol. 37, no. 34, pp. 3192-3202, Dec 1 2019, doi: 10.1200/JCO.19.00915.

[26] M. E. Dudley, J. R. Wunderlich, P. F. Robbins, J. C. Yang, P. Hwu, D. J. Schwartzentruber, S. L. Topalian, R. Sherry, N. P. Restifo, A. M. Hubicki, M. R. Robinson, M. Raffeld, P. Duray, C. A. Seipp, L. Rogers-Freezer, K. E. Morton, S. A. Mavroukakis, D. E. White, and S. A. Rosenberg, "Cancer regression and autoimmunity in patients after clonal repopulation with antitumor lymphocytes," *Science,* vol. 298, no. 5594, pp. 850-4, Oct 25 2002, doi: 10.1126/science.1076514.

[27] J. Dunst, S. Ahrens, M. Paulussen, S. Burdach, and H. Jurgens, "Prognostic impact of tumor perfusion in MR-imaging studies in Ewing tumors," *Strahlenther Onkol,* vol. 177, no. 3, pp. 153-9, Mar 2001, doi: 10.1007/s00066-001-0804-8.

[28] M. Ehnman, W. Chaabane, F. Haglund, and P. Tsagkozis, "The Tumor Microenvironment of Pediatric Sarcoma: Mesenchymal Mechanisms Regulating Cell Migration and Metastasis," *Curr Oncol Rep,* vol. 21, no. 10, p. 90, Aug 15 2019, doi: 10.1007/s11912-019-0839-6.

[29] D. J. Elzi, M. Song, P. J. Houghton, Y. Chen, and Y. Shiio, "The role of FLI-1-EWS, a fusion gene reciprocal to EWS-FLI-1, in Ewing sarcoma," *Genes Cancer,* vol. 6, no. 11-12, pp. 452-61, Nov 2015, doi: 10.18632/genesandcancer.86.

[30] N. J. Felix and P. M. Allen, "Specificity of T-cell alloreactivity," *Nat Rev Immunol,* vol. 7, no. 12, pp. 942-53, Dec 2007, doi: 10.1038/nri2200.

[31] A. Ferrari, U. Dirksen, and S. Bielack, "Sarcomas of Soft Tissue and Bone," *Prog Tumor Res,* vol. 43, pp. 128-41, 2016, doi: 10.1159/000447083.

[32] C. Fu and A. Jiang, "Dendritic Cells and CD8 T Cell Immunity in Tumor Microenvironment," *Front Immunol,* vol. 9, p. 3059, 2018, doi: 10.3389/fimmu.2018.03059.

[33] Y. Fujimoto, L. Tu, A. S. Miller, C. Bock, M. Fujimoto, C. Doyle, D. A. Steeber, and T. F. Tedder, "CD83 expression influences CD4+ T cell development in the thymus," *Cell,* vol. 108, no. 6, pp. 755-67, Mar 22 2002, doi: 10.1016/s0092-8674(02)00673-6.

[34] T. Fujiwara, J. Fukushi, S. Yamamoto, Y. Matsumoto, N. Setsu, Y. Oda, H. Yamada, S. Okada, K. Watari, M. Ono, M. Kuwano, S. Kamura, K. Iida, Y. Okada, M. Koga, and Y. Iwamoto, "Macrophage infiltration predicts a poor prognosis for human ewing sarcoma," *Am J Pathol,* vol. 179, no. 3, pp. 1157-70, Sep 2011, doi: 10.1016/j.ajpath.2011.05.034.

[35] F. Garrido, F. Ruiz-Cabello, and N. Aptsiauri, "Rejection versus escape: the tumor MHC dilemma," *Cancer Immunol Immunother,* vol. 66, no. 2, pp. 259-271, Feb 2017, doi: 10.1007/s00262-016-1947-x.

[36] A. W. Goldrath and M. J. Bevan, "Selecting and maintaining a diverse T-cell repertoire," *Nature,* vol. 402, no. 6759, pp. 255-62, Nov 18 1999, doi: 10.1038/46218.

[37] H. E. Grier, "The Ewing family of tumors. Ewing's sarcoma and primitive neuroectodermal tumors," *Pediatr Clin North Am,* vol. 44, no. 4, pp. 991-1004, Aug 1997, doi: 10.1016/s0031-3955(05)70541-1.

[38] S. N. Grobner, B. C. Worst, J. Weischenfeldt, I. Buchhalter, K. Kleinheinz, V. A. Rudneva, P. D. Johann, G. P. Balasubramanian, M. Segura-Wang, S. Brabetz, S. Bender, B. Hutter, D. Sturm, E. Pfaff, D. Hubschmann, G. Zipprich, M. Heinold, J. Eils, C. Lawerenz, S. Erkek, S. Lambo, S. Waszak, C. Blattmann, A. Borkhardt, M. Kuhlen, A. Eggert, S. Fulda, M. Gessler, J. Wegert, R. Kappler, D. Baumhoer, S. Burdach, R. Kirschner-Schwabe, U. Kontny, A. E. Kulozik, D. Lohmann, S. Hettmer, C. Eckert, S. Bielack, M. Nathrath, C. Niemeyer, G. H. Richter, J. Schulte, R. Siebert, F. Westermann, J. J. Molenaar, G. Vassal, H. Witt, I. P.-S. Project, I. M.-S. Project, B. Burkhardt, C. P. Kratz, O. Witt, C. M. van Tilburg, C. M. Kramm, G. Fleischhack, U. Dirksen, S. Rutkowski, M. Fruhwald, K. von Hoff, S. Wolf, T. Klingebiel, E. Koscielniak, P. Landgraf, J. Koster, A. C. Resnick, J. Zhang, Y. Liu, X. Zhou, A. J. Waanders, D. A. Zwijnenburg, P. Raman, B. Brors, U. D. Weber, P. A. Northcott, K. W. Pajtler, M. Kool, R. M. Piro, J. O. Korbel, M. Schlesner, R. Eils, D. T. W. Jones, P. Lichter, L. Chavez, M. Zapatka, and S. M. Pfister, "The landscape of genomic alterations across childhood cancers," *Nature,* vol. 555, no. 7696, pp. 321-327, Mar 15 2018, doi: 10.1038/nature25480.

[39] L. Grosche, I. Knippertz, C. Konig, D. Royzman, A. B. Wild, E. Zinser, H. Sticht, Y. A. Muller, A. Steinkasserer, and M. Lechmann, "The CD83 Molecule - An Important Immune Checkpoint," *Front Immunol,* vol. 11, p. 721, 2020, doi: 10.3389/fimmu.2020.00721.

[40] J. L. Guerriero, "Macrophages: Their Untold Story in T Cell Activation and Function," *Int Rev Cell Mol Biol,* vol. 342, pp. 73-93, 2019, doi: 10.1016/bs.ircmb.2018.07.001.

[41] J. Haeusler, A. Ranft, T. Boelling, G. Gosheger, G. Braun-Munzinger, V. Vieth, S. Burdach, H. van den Berg, H. Juergens, and U. Dirksen, "The value of local treatment in patients with primary, disseminated, multifocal Ewing sarcoma (PDMES)," *Cancer,* vol. 116, no. 2, pp. 443-50, Jan 15 2010, doi: 10.1002/cncr.24740.

[42] H. Hamidi, J. Lilja, and J. Ivaska, "Using xCELLigence RTCA Instrument to Measure Cell Adhesion," *Bio Protoc,* vol. 7, no. 24, Dec 20 2017, doi: 10.21769/BioProtoc.2646.

[43] D. C. Hinshaw and L. A. Shevde, "The Tumor Microenvironment Innately Modulates Cancer Progression," *Cancer Res,* vol. 79, no. 18, pp. 4557-4566, Sep 15 2019, doi: 10.1158/0008-5472.CAN-18-3962.

[44] Y. Hiraki, H. Inoue, K. Iyama, A. Kamizono, M. Ochiai, C. Shukunami, S. Iijima, F. Suzuki, and J. Kondo, "Identification of chondromodulin I as a novel endothelial cell growth inhibitor. Purification and its localization in the avascular zone of epiphyseal cartilage," *J Biol Chem,* vol. 272, no. 51, pp. 32419-26, Dec 19 1997, doi: 10.1074/jbc.272.51.32419.

[45] Y. Hiraki, H. Tanaka, H. Inoue, J. Kondo, A. Kamizono, and F. Suzuki, "Molecular cloning of a new class of cartilage-specific matrix, chondromodulin-I, which stimulates growth of cultured chondrocytes," *Biochem Biophys Res Commun,* vol. 175, no. 3, pp. 971-7, Mar 29 1991, doi: 10.1016/0006-291x(91)91660-5.

[46] N. Hirano, M. O. Butler, Z. Xia, S. Ansen, M. S. von Bergwelt-Baildon, D. Neuberg, G. J. Freeman, and L. M. Nadler, "Engagement of CD83 ligand induces prolonged expansion of CD8+ T cells and preferential enrichment for antigen specificity," *Blood,* vol. 107, no. 4, pp. 1528-36, Feb 15 2006, doi: 10.1182/blood-2005-05-2073.

[47] J. M. Horvatinovich, E. W. Grogan, M. Norris, A. Steinkasserer, H. Lemos, A. L. Mellor, I. Y. Tcherepanova, C. A. Nicolette, and M. A. DeBenedette, "Soluble CD83 Inhibits T Cell Activation by Binding to the TLR4/MD-2 Complex on CD14(+) Monocytes," *J Immunol,* vol. 198, no. 6, pp. 2286-2301, Mar 15 2017, doi: 10.4049/jimmunol.1600802.

[48] S. Hoving, A. L. Seynhaeve, S. T. van Tiel, G. aan de Wiel-Ambagtsheer, E. A. de Bruijn, A. M. Eggermont, and T. L. ten Hagen, "Early destruction of tumor vasculature in tumor necrosis factor-alpha-based isolated limb perfusion is responsible for tumor response," *Anticancer Drugs,* vol. 17, no. 8, pp. 949-59, Sep 2006, doi: 10.1097/01.cad.0000224450.54447.b3.

[49] H. T. Idriss and J. H. Naismith, "TNF alpha and the TNF receptor superfamily: structure-function relationship(s)," *Microsc. Res. Tech.,* vol. 50, no. 3, pp. 184-95, Aug 1 2000, doi: 10.1002/1097-0029(20000801)50:3<184::AID-JEMT2>3.0.CO;2-H.

[50] Y. Inagaki, E. Hookway, K. A. Williams, A. B. Hassan, U. Oppermann, Y. Tanaka, E. Soilleux, and N. A. Athanasou, "Dendritic and mast cell involvement in the inflammatory response to primary malignant bone tumours," *Clin Sarcoma Res,* vol. 6, p. 13, 2016, doi: 10.1186/s13569-016-0053-3.

[51] S. F. Josephs, T. E. Ichim, S. M. Prince, S. Kesari, F. M. Marincola, A. R. Escobedo, and A. Jafri, "Unleashing endogenous TNF-alpha as a cancer immunotherapeutic," *J Transl Med,* vol. 16, no. 1, p. 242, Aug 31 2018, doi: 10.1186/s12967-018-1611-7.

[52] S. Kailayangiri, B. Altvater, S. Lesch, S. Balbach, C. Gottlich, J. Kuhnemundt, J. H. Mikesch, S. Schelhaas, S. Jamitzky, J. Meltzer, N. Farwick, L. Greune, M. Fluegge, K. Kerl, H. N. Lode, N. Siebert, I. Muller, H. Walles, W. Hartmann, and C. Rossig, "EZH2 Inhibition in Ewing Sarcoma Upregulates GD2 Expression for Targeting with Gene-Modified T Cells," *Mol Ther,* vol. 27, no. 5, pp. 933-946, May 8 2019, doi: 10.1016/j.ymthe.2019.02.014.

[53] N. Karadurmus, U. Sahin, B. Bahadir Basgoz, and T. Demirer, "Is there a role of high dose chemotherapy and autologous stem cell transplantation in the treatment of Ewing's sarcoma and osteosarcomas?," *J BUON,* vol. 23, no. 5, pp. 1235-1241, Sep-Oct 2018. [Online]. Available: https://www.ncbi.nlm.nih.gov/pubmed/30570842.

[54] Kinderkrebsinfo. "Ewing 2008." https://www.kinderkrebsinfo.de/fachinformationen/studienportal/pohkinderkrebsinfotherapiestudien/ewing_2008/index_ger.html (accessed.

[55] H. J. Kolb, "Graft-versus-leukemia effects of transplantation and donor lymphocytes," *Blood,* vol. 112, no. 12, pp. 4371-83, Dec 1 2008, doi: 10.1182/blood-2008-03-077974.

[56] H. Kovar, "Blocking the road, stopping the engine or killing the driver? Advances in targeting EWS/FLI-1 fusion in Ewing sarcoma as novel therapy," *Expert Opin Ther Targets,* vol. 18, no. 11, pp. 1315-28, Nov 2014, doi: 10.1517/14728222.2014.947963.

[57] B. Kretschmer, K. Luthje, A. H. Guse, S. Ehrlich, F. Koch-Nolte, F. Haag, B. Fleischer, and M. Breloer, "CD83 modulates B cell function in vitro: increased IL-10 and reduced Ig secretion by CD83Tg B cells," *PLoS One,* vol. 2, no. 8, p. e755, Aug 15 2007, doi: 10.1371/journal.pone.0000755.

[58] M. Lechmann, E. Zinser, A. Golka, and A. Steinkasserer, "Role of CD83 in the immunomodulation of dendritic cells," *Int Arch Allergy Immunol,* vol. 129, no. 2, pp. 113-8, Oct 2002, doi: 10.1159/000065883.

[59] S. L. Lessnick and M. Ladanyi, "Molecular pathogenesis of Ewing sarcoma: new therapeutic and transcriptional targets," *Annu Rev Pathol,* vol. 7, pp. 145-59, 2012, doi: 10.1146/annurev-pathol-011110-130237.

[60] Z. Li, X. Ju, P. A. Silveira, E. Abadir, W. H. Hsu, D. N. J. Hart, and G. J. Clark, "CD83: Activation Marker for Antigen Presenting Cells and Its Therapeutic Potential," *Front Immunol,* vol. 10, p. 1312, 2019, doi: 10.3389/fimmu.2019.01312.

[61] D. Lienard, P. Ewalenko, J. J. Delmotte, N. Renard, and F. J. Lejeune, "High-dose recombinant tumor necrosis factor alpha in combination with interferon gamma and melphalan in isolation perfusion of the limbs for melanoma and sarcoma," *J Clin Oncol,* vol. 10, no. 1, pp. 52-60, Jan 1992, doi: 10.1200/JCO.1992.10.1.52.

[62] X. Lin, L. Wang, and F. Wang, "ChondromodulinI suppresses tumorigenesis of human osteosarcoma cells," *Mol Med Rep,* vol. 16, no. 6, pp. 8542-8548, Dec 2017, doi: 10.3892/mmr.2017.7629.

[63] H. Liu, R. Jain, J. Guan, V. Vuong, S. Ishido, N. L. La Gruta, D. H. Gray, J. A. Villadangos, and J. D. Mintern, "Ubiquitin ligase MARCH 8 cooperates with CD83 to control surface MHC II expression in thymic epithelium and CD4 T cell selection," *J Exp Med,* vol. 213, no. 9, pp. 1695-703, Aug 22 2016, doi: 10.1084/jem.20160312.

[64] C. Mackintosh, J. Madoz-Gurpide, J. L. Ordonez, D. Osuna, and D. Herrero-Martin, "The molecular pathogenesis of Ewing's sarcoma," *Cancer Biol Ther,* vol. 9, no. 9, pp. 655-67, May 1 2010, doi: 10.4161/cbt.9.9.11511.

[65] K. Maeda, S. M. Kang, T. Sawada, Y. Nishiguchi, M. Yashiro, Y. Ogawa, M. Ohira, T. Ishikawa, and Y. S. C. K. Hirakawa, "Expression of intercellular adhesion molecule-1 and prognosis in colorectal cancer," *Oncol Rep,* vol. 9, no. 3, pp. 511-4, May-Jun 2002. [Online]. Available: https://www.ncbi.nlm.nih.gov/pubmed/11956618.

[66] G. Mathe, J. L. Amiel, L. Schwarzenberg, A. Cattan, and M. Schneider, "Adoptive immunotherapy of acute leukemia: experimental and clinical results," *Cancer Res,* vol. 25, no. 9, pp. 1525-31, Oct 1965. [Online]. Available: https://www.ncbi.nlm.nih.gov/pubmed/5323965.

[67] T. A. McKinsey, Z. Chu, T. F. Tedder, and D. W. Ballard, "Transcription factor NF-kappaB regulates inducible CD83 gene expression in activated T lymphocytes," *Mol Immunol,* vol. 37, no. 12-13, pp. 783-8, Aug-Sep 2000, doi: 10.1016/s0161-5890(00)00099-7.

[68] E. Morales, M. Olson, F. Iglesias, S. Dahiya, T. Luetkens, and D. Atanackovic, "Role of immunotherapy in Ewing sarcoma," *J Immunother Cancer,* vol. 8, no. 2, Dec 2020, doi: 10.1136/jitc-2020-000653.

[69] H. Nie, Y. Zheng, R. Li, T. B. Guo, D. He, L. Fang, X. Liu, L. Xiao, X. Chen, B. Wan, Y. E. Chin, and J. Z. Zhang, "Phosphorylation of FOXP3 controls regulatory T cell function and is inhibited by TNF-alpha in rheumatoid arthritis," *Nat Med,* vol. 19, no. 3, pp. 322-8, Mar 2013, doi: 10.1038/nm.3085.

[70] K. Papamichael, S. Lin, M. Moore, G. Papaioannou, L. Sattler, and A. S. Cheifetz, "Infliximab in inflammatory bowel disease," *Ther Adv Chronic Dis,* vol. 10, p. 2040622319838443, 2019, doi: 10.1177/2040622319838443.

[71] A. S. Pappo and U. Dirksen, "Rhabdomyosarcoma, Ewing Sarcoma, and Other Round Cell Sarcomas," *J Clin Oncol,* vol. 36, no. 2, pp. 168-179, Jan 10 2018, doi: 10.1200/JCO.2017.74.7402.

[72] C. M. Prazma and T. F. Tedder, "Dendritic cell CD83: a therapeutic target or innocent bystander?," *Immunol Lett,* vol. 115, no. 1, pp. 1-8, Jan 15 2008, doi: 10.1016/j.imlet.2007.10.001.

[73] A. T. Prechtel and A. Steinkasserer, "CD83: an update on functions and prospects of the maturation marker of dendritic cells," *Arch Dermatol Res,* vol. 299, no. 2, pp. 59-69, May 2007, doi: 10.1007/s00403-007-0743-z.

[74] L. J. Qin, T. Zhang, Y. S. Jia, Y. B. Zhang, Y. X. Zhang, and H. T. Wang, "Thermotherapy-induced reduction in glioma invasiveness is mediated by tumor necrosis factor-alpha," *Genet Mol Res,* vol. 14, no. 4, pp. 11771-9, Oct 2 2015, doi: 10.4238/2015.October.2.11.

[75] M. Reina and E. Espel, "Role of LFA-1 and ICAM-1 in Cancer," *Cancers (Basel),* vol. 9, no. 11, Nov 3 2017, doi: 10.3390/cancers9110153.

[76] G. H. Richter, S. Plehm, A. Fasan, S. Rossler, R. Unland, I. M. Bennani-Baiti, M. Hotfilder, D. Lowel, I. von Luettichau, I. Mossbrugger, L. Quintanilla-Martinez, H. Kovar, M. S. Staege, C. Muller-Tidow, and S. Burdach, "EZH2 is a mediator of EWS/FLI1 driven tumor growth and metastasis blocking endothelial and neuro-ectodermal differentiation," *Proc. Natl. Acad. Sci. U. S. A.,* vol. 106, no. 13, pp. 5324-9, Mar 31 2009, doi: 10.1073/pnas.0810759106.

[77] K. A. Roebuck and A. Finnegan, "Regulation of intercellular adhesion molecule-1 (CD54) gene expression," *J Leukoc Biol,* vol. 66, no. 6, pp. 876-88, Dec 1999, doi: 10.1002/jlb.66.6.876.

[78] M. W. Rohaan, S. Wilgenhof, and J. Haanen, "Adoptive cellular therapies: the current landscape," *Virchows Arch,* vol. 474, no. 4, pp. 449-461, Apr 2019, doi: 10.1007/s00428-018-2484-0.

[79] S. A. Rosenberg, B. S. Packard, P. M. Aebersold, D. Solomon, S. L. Topalian, S. T. Toy, P. Simon, M. T. Lotze, J. C. Yang, C. A. Seipp, and et al., "Use of tumor-infiltrating lymphocytes and interleukin-2 in the immunotherapy of patients with metastatic melanoma. A preliminary report," *N Engl J Med,* vol. 319, no. 25, pp. 1676-80, Dec 22 1988, doi: 10.1056/NEJM198812223192527.

[80] K. C. Roy, G. Bandyopadhyay, S. Rakshit, M. Ray, and S. Bandyopadhyay, "IL-4 alone without the involvement of GM-CSF transforms human peripheral blood monocytes to a CD1a(dim), CD83(+) myeloid dendritic cell subset," *J Cell Sci,* vol. 117, no. Pt 16, pp. 3435-45, Jul 15 2004, doi: 10.1242/jcs.01162.

[81] C. E. Rube, F. van Valen, F. Wilfert, J. Palm, A. Schuck, N. Willich, W. Winkelmann, H. Jurgens, and C. Rube, "Ewing's sarcoma and peripheral primitive neuroectodermal tumor cells produce large quantities of bioactive tumor necrosis factor-alpha (TNF-alpha) after radiation exposure," *Int J Radiat Oncol Biol Phys,* vol. 56, no. 5, pp. 1414-25, Aug 1 2003, doi: 10.1016/s0360-3016(03)00418-8.

[82] M. Salio, M. Cella, M. Suter, and A. Lanzavecchia, "Inhibition of dendritic cell maturation by herpes simplex virus," *Eur J Immunol,* vol. 29, no. 10, pp. 3245-53, Oct 1999, doi: 10.1002/(SICI)1521-4141(199910)29:10<3245::AID-IMMU3245>3.0.CO;2-X.

[83] R. D. Schreiber, L. J. Old, and M. J. Smyth, "Cancer immunoediting: integrating immunity's roles in cancer suppression and promotion," *Science,* vol. 331, no. 6024, pp. 1565-70, Mar 25 2011, doi: 10.1126/science.1203486.

[84] K. Scotlandi, C. M. Hattinger, E. Pellegrini, M. Gambarotti, and M. Serra, "Genomics and Therapeutic Vulnerabilities of Primary Bone Tumors," *Cells,* vol. 9, no. 4, Apr 14 2020, doi: 10.3390/cells9040968.

[85] G. Sethi, B. Sung, and B. B. Aggarwal, "TNF: a master switch for inflammation to cancer," *Front Biosci,* vol. 13, pp. 5094-107, May 1 2008, doi: 10.2741/3066.
[86] A. H. Sharpe and K. E. Pauken, "The diverse functions of the PD1 inhibitory pathway," *Nat Rev Immunol,* vol. 18, no. 3, pp. 153-167, Mar 2018, doi: 10.1038/nri.2017.108.
[87] J. S. Shin, M. Ebersold, M. Pypaert, L. Delamarre, A. Hartley, and I. Mellman, "Surface expression of MHC class II in dendritic cells is controlled by regulated ubiquitination," *Nature,* vol. 444, no. 7115, pp. 115-8, Nov 2 2006, doi: 10.1038/nature05261.
[88] G. Spitaleri, R. Berardi, C. Pierantoni, T. De Pas, C. Noberasco, C. Libbra, R. Gonzalez-Iglesias, L. Giovannoni, A. Tasciotti, D. Neri, H. D. Menssen, and F. de Braud, "Phase I/II study of the tumour-targeting human monoclonal antibody-cytokine fusion protein L19-TNF in patients with advanced solid tumours," *J Cancer Res Clin Oncol,* vol. 139, no. 3, pp. 447-55, Mar 2013, doi: 10.1007/s00432-012-1327-7.
[89] C. Spurny, S. Kailayangiri, S. Jamitzky, B. Altvater, E. Wardelmann, U. Dirksen, J. Hardes, W. Hartmann, and C. Rossig, "Programmed cell death ligand 1 (PD-L1) expression is not a predominant feature in Ewing sarcomas," *Pediatr Blood Cancer,* vol. 65, no. 1, Jan 2018, doi: 10.1002/pbc.26719.
[90] M. S. Staege, C. Hutter, I. Neumann, S. Foja, U. E. Hattenhorst, G. Hansen, D. Afar, and S. E. Burdach, "DNA microarrays reveal relationship of Ewing family tumors to both endothelial and fetal neural crest-derived cells and define novel targets," *Cancer Res,* vol. 64, no. 22, pp. 8213-21, Nov 15 2004, doi: 10.1158/0008-5472.CAN-03-4059.
[91] D. Stahl, A. J. Gentles, R. Thiele, and I. Gutgemann, "Prognostic profiling of the immune cell microenvironment in Ewing s Sarcoma Family of Tumors," *Oncoimmunology,* vol. 8, no. 12, p. e1674113, 2019, doi: 10.1080/2162402X.2019.1674113.
[92] Y. Tai, Q. Wang, H. Korner, L. Zhang, and W. Wei, "Molecular Mechanisms of T Cells Activation by Dendritic Cells in Autoimmune Diseases," *Front Pharmacol,* vol. 9, p. 642, 2018, doi: 10.3389/fphar.2018.00642.
[93] H. A. Tawbi, M. Burgess, V. Bolejack, B. A. Van Tine, S. M. Schuetze, J. Hu, S. D'Angelo, S. Attia, R. F. Riedel, D. A. Priebat, S. Movva, L. E. Davis, S. H. Okuno, D. R. Reed, J. Crowley, L. H. Butterfield, R. Salazar, J. Rodriguez-Canales, A. J. Lazar, Wistuba, II, L. H. Baker, R. G. Maki, D. Reinke, and S. Patel, "Pembrolizumab in advanced soft-tissue sarcoma and bone sarcoma (SARC028): a multicentre, two-cohort, single-arm, open-label, phase 2 trial," *Lancet Oncol,* vol. 18, no. 11, pp. 1493-1501, Nov 2017, doi: 10.1016/S1470-2045(17)30624-1.
[94] U. Thiel, S. Pirson, C. Muller-Spahn, H. Conrad, D. H. Busch, H. Bernhard, S. Burdach, and G. H. Richter, "Specific recognition and inhibition of Ewing tumour growth by antigen-specific allo-restricted cytotoxic T cells," *Br J Cancer,* vol. 104, no. 6, pp. 948-56, Mar 15 2011, doi: 10.1038/bjc.2011.54.
[95] U. Thiel, S. J. Schober, I. Einspieler, A. Kirschner, M. Thiede, D. Schirmer, K. Gall, F. Blaeschke, O. Schmidt, S. Jabar, A. Ranft, R. Alba Rubio, U. Dirksen, T. G. P. Grunewald, P. H. Sorensen, G. H. S. Richter, I. T. von Luttichau, D. H. Busch, and S. E. G. Burdach, "Ewing sarcoma partial regression without GvHD by chondromodulin-I/HLA-A*02:01-specific allorestricted T cell receptor transgenic T cells," *Oncoimmunology,* vol. 6, no. 5, p. e1312239, 2017, doi: 10.1080/2162402X.2017.1312239.
[96] U. Thiel, A. Wawer, P. Wolf, M. Badoglio, A. Santucci, T. Klingebiel, O. Basu, A. Borkhardt, H. J. Laws, Y. Kodera, A. Yoshimi, C. Peters, R. Ladenstein, A. Pession, A. Prete, E. C. Urban, W. Schwinger, P. Bordigoni, A. Salmon, M. A. Diaz, B. Afanasyev, I.

Lisukov, E. Morozova, A. Toren, B. Bielorai, J. Korsakas, F. Fagioli, D. Caselli, G. Ehninger, B. Gruhn, U. Dirksen, F. Abdel-Rahman, M. Aglietta, E. Mastrodicasa, M. Torrent, P. Corradini, F. Demeocq, G. Dini, P. Dreger, M. Eyrich, J. Gozdzik, F. Guilhot, E. Holler, E. Koscielniak, C. Messina, D. Nachbaur, R. Sabbatini, E. Oldani, H. Ottinger, H. Ozsahin, R. Schots, S. Siena, J. Stein, S. Sufliarska, A. Unal, M. Ussowicz, P. Schneider, W. Woessmann, H. Jurgens, M. Bregni, S. Burdach, P. Solid Tumor Working, B. the Pediatric DiseaseWorking Party of the European Group for, T. Marrow, B. Asia Pacific, T. Marrow, T. Pediatric Registry for Stem Cell, and E. S. G. Meta, "No improvement of survival with reduced- versus high-intensity conditioning for allogeneic stem cell transplants in Ewing tumor patients," *Ann Oncol,* vol. 22, no. 7, pp. 1614-21, Jul 2011, doi: 10.1093/annonc/mdq703.

[97] F. Tirode, D. Surdez, X. Ma, M. Parker, M. C. Le Deley, A. Bahrami, Z. Zhang, E. Lapouble, S. Grossetete-Lalami, M. Rusch, S. Reynaud, T. Rio-Frio, E. Hedlund, G. Wu, X. Chen, G. Pierron, O. Oberlin, S. Zaidi, G. Lemmon, P. Gupta, B. Vadodaria, J. Easton, M. Gut, L. Ding, E. R. Mardis, R. K. Wilson, S. Shurtleff, V. Laurence, J. Michon, P. Marec-Berard, I. Gut, J. Downing, M. Dyer, J. Zhang, O. Delattre, P. St. Jude Children's Research Hospital-Washington University Pediatric Cancer Genome, and C. the International Cancer Genome, "Genomic landscape of Ewing sarcoma defines an aggressive subtype with co-association of STAG2 and TP53 mutations," *Cancer Discov,* vol. 4, no. 11, pp. 1342-53, Nov 2014, doi: 10.1158/2159-8290.CD-14-0622.

[98] E. C. Toomey, J. D. Schiffman, and S. L. Lessnick, "Recent advances in the molecular pathogenesis of Ewing's sarcoma," *Oncogene,* vol. 29, no. 32, pp. 4504-16, Aug 12 2010, doi: 10.1038/onc.2010.205.

[99] L. E. Tze, K. Horikawa, H. Domaschenz, D. R. Howard, C. M. Roots, R. J. Rigby, D. A. Way, M. Ohmura-Hoshino, S. Ishido, C. E. Andoniou, M. A. Degli-Esposti, and C. C. Goodnow, "CD83 increases MHC II and CD86 on dendritic cells by opposing IL-10-driven MARCH1-mediated ubiquitination and degradation," *J Exp Med,* vol. 208, no. 1, pp. 149-65, Jan 17 2011, doi: 10.1084/jem.20092203.

[100] F. van Valen, V. Kentrup-Lardong, B. Truckenbrod, C. Rube, W. Winkelmann, and W. W. Jurgens, "Regulation of the release of tumour necrosis factor (TNF)alpha and soluble TNF receptor by gamma irradiation and interferon gamma in Ewing's sarcoma/peripheral primitive neuroectodermal tumour cells," *J Cancer Res Clin Oncol,* vol. 123, no. 5, pp. 245-52, 1997, doi: 10.1007/BF01208634.

[101] R. Veenstra, M. Kostine, A. M. Cleton-Jansen, N. F. de Miranda, and J. V. Bovee, "Immune checkpoint inhibitors in sarcomas: in quest of predictive biomarkers," *Lab Invest,* vol. 98, no. 1, pp. 41-50, Jan 2018, doi: 10.1038/labinvest.2017.128.

[102] Z. Vegh, P. Wang, F. Vanky, and E. Klein, "Increased expression of MHC class I molecules on human cells after short time IFN-gamma treatment," *Mol Immunol,* vol. 30, no. 9, pp. 849-54, Jun 1993, doi: 10.1016/0161-5890(93)90008-y.

[103] K. von Heyking, J. Calzada-Wack, S. Gollner, F. Neff, O. Schmidt, T. Hensel, D. Schirmer, A. Fasan, I. Esposito, C. Muller-Tidow, P. H. Sorensen, S. Burdach, and G. H. S. Richter, "The endochondral bone protein CHM1 sustains an undifferentiated, invasive phenotype, promoting lung metastasis in Ewing sarcoma," *Mol Oncol,* vol. 11, no. 9, pp. 1288-1301, Sep 2017, doi: 10.1002/1878-0261.12057.

[104] J. von Rohrscheidt, E. Petrozziello, J. Nedjic, C. Federle, L. Krzyzak, H. L. Ploegh, S. Ishido, A. Steinkasserer, and L. Klein, "Thymic CD4 T cell selection requires attenuation of March8-mediated MHCII turnover in cortical epithelial cells through

CD83," *J Exp Med,* vol. 213, no. 9, pp. 1685-94, Aug 22 2016, doi: 10.1084/jem.20160316.

[105] J. Whelan, M. C. Le Deley, U. Dirksen, G. Le Teuff, B. Brennan, N. Gaspar, D. S. Hawkins, S. Amler, S. Bauer, S. Bielack, J. Y. Blay, S. Burdach, M. P. Castex, D. Dilloo, A. Eggert, H. Gelderblom, J. C. Gentet, W. Hartmann, W. A. Hassenpflug, L. Hjorth, M. Jimenez, T. Klingebiel, U. Kontny, J. Kruseova, R. Ladenstein, V. Laurence, C. Lervat, P. Marec-Berard, S. Marreaud, J. Michon, B. Morland, M. Paulussen, A. Ranft, P. Reichardt, H. van den Berg, K. Wheatley, I. Judson, I. Lewis, A. Craft, H. Juergens, O. Oberlin, E. W. I. N. G. Euro, and E.-. Investigators, "High-Dose Chemotherapy and Blood Autologous Stem-Cell Rescue Compared With Standard Chemotherapy in Localized High-Risk Ewing Sarcoma: Results of Euro-E.W.I.N.G.99 and Ewing-2008," *J Clin Oncol,* p. JCO2018782516, Sep 6 2018, doi: 10.1200/JCO.2018.78.2516.

[106] H. Yabe, T. Tsukahara, S. Kawaguchi, T. Wada, T. Torigoe, N. Sato, C. Terai, M. Aoki, S. Hirose, H. Morioka, and H. Yabe, "Prognostic significance of HLA class I expression in Ewing's sarcoma family of tumors," *J Surg Oncol,* vol. 103, no. 5, pp. 380-5, Apr 2011, doi: 10.1002/jso.21829.

[107] F. Zhou, "Molecular mechanisms of IFN-gamma to up-regulate MHC class I antigen processing and presentation," *Int Rev Immunol,* vol. 28, no. 3-4, pp. 239-60, 2009, doi: 10.1080/08830180902978120.

[108] L. J. Zhou, R. Schwarting, H. M. Smith, and T. F. Tedder, "A novel cell-surface molecule expressed by human interdigitating reticulum cells, Langerhans cells, and activated lymphocytes is a new member of the Ig superfamily," *J Immunol,* vol. 149, no. 2, pp. 735-42, Jul 15 1992. [Online]. Available: https://www.ncbi.nlm.nih.gov/pubmed/1378080.

[109] M. M. T. Zhu, E. Shenasa, and T. O. Nielsen, "Sarcomas: Immune biomarker expression and checkpoint inhibitor trials," *Cancer Treat Rev,* vol. 91, p. 102115, Dec 2020, doi: 10.1016/j.ctrv.2020.102115.

[110] S. Zhu, H. Qiu, S. Bennett, V. Kuek, V. Rosen, H. Xu, and J. Xu, "Chondromodulin-1 in health, osteoarthritis, cancer, and heart disease," *Cell Mol Life Sci,* vol. 76, no. 22, pp. 4493-4502, Nov 2019, doi: 10.1007/s00018-019-03225-y.